Chaos, Solitons and Fractals 000 (2019) 1–16

Contents lists available at ScienceDirect

Chaos, Solitons and Fractals

Nonlinear Science, and Nonequilibrium and Complex Phenomena

journal homepage: www.elsevier.com/locate/chaos

# Explicit impacts of harvesting in delayed predator-prey models

Binandita Barman, Bapan Ghosh*

*Department of Mathematics, National Institute of Technology Meghalaya, Shillong, Meghalaya 793003, India*

ARTICLE INFO

*Article history:*
Received 29 October 2018
Revised 1 March 2019
Accepted 2 March 2019
Available online xxx

*Keywords:*
Delay differential equation
Stability switching
Population dynamics
Harvesting

ABSTRACT

Modeling population dynamics using delay differential equations and exploring the impacts of harvesting in predator-prey systems are among few of the thrust areas of research in theoretical and applied ecology. Many results are established to understand distinct dynamics under population harvesting. However, comparatively less attention is paid to explain the explicit harvesting effects when populations fluctuate due to time delay. In this contribution, two well known Lotka–Volterra (LV) type and Rosenzweig–MacArthur (RM) predator-prey models incorporating time delay into the logistic growth term are considered. The analysis and the obtained results are summarized as follows. (a) Firstly, the dynamics of both the models, by considering the time delay as the bifurcation parameter, is analyzed. Some of the parameter conditions for the delay induced stability switching are improved and corrected in comparison to the earlier works. The delay induced stability results are derived and found to be similar for both the models. (b) We investigate whether harvesting of either prey or predator can locally stabilize (respectively, destabilize) the system when the unharvested system dynamics is at non-equilibrium (respectively, stable steady state) mode due to time delay. It is observed that harvesting can induce stability and instability switching depending upon the dynamics mode of the unharvested system. (c) In the same framework, we examine if a stable steady state can be obtained when predator is harvested towards Maximum Sustainable Yield (MSY) level. Unlike the case of non-delayed LV type and RM predator-prey models, it is found that harvesting the predator towards MSY in the delayed models does not guarantee a stable stock. The new results compared to the existing literature might contribute in enriching fishery management policy and theoretical ecology as a whole.



## 1. Introduction

Understanding interaction between species and analyzing various dynamical behavior using conceptual models is one of the fascinated areas of research in theoretical ecology. In particular, many mathematical models of single and multi-species system are used for describing fishery regulation and sustainability in fishery managements. Accordingly, many fishery management tools viz. MSY policy [3,37,45], *Maximum Economic Yield* (MEY) policy [50], *Pretty Good Yield* (PGY) policy [16], *Ecosystem Based Fisheries Management* [41], *Marine Protected Areas* (MPAs) [12,23] had been developed. The above contributions including [6,8,11,28,36], etc., considered models where populations persist at a globally stable steady state.

However, populations can also coexist in the form of non-equilibrium states due to environmental fluctuation, human activity or because of inherent species interaction. Hence, oscillations and chaotic dynamics are common in ecological systems. Oscillation may arise in Rosenzweig–MacArthur predator-prey system whereas tri-trophic food chain exhibits chaotic dynamics [1,15,25]. Such oscillations or the chaotic dynamics are modeled by taking account of Holling type II functional responses. Ghosh et al. [10] and Tromeur and Loeuille [51] have shown that harvesting either prey or predator can remove oscillations from Rosenzweig–MacArthur predator-prey model. In addition, Ghosh et al. [10] established that system becomes stable when predator is exploited at optimum level. Very recently, Ghosh et al. [13] studied a tri-trophic food chain and concluded that harvesting top-predator may cause instability in the system.

Time delay is very important in modeling any physical, biological or engineering problems. For example, $\tau$ (time delay) is the estimated time for a larva to get matured into adult (butterfly). Since they are cultivated within limited resources, the competition within species for limited resources at current time $t$ will be modeled not only by the adult population at time $t$ but also by the newly formed adult population at time $(t-\tau)$. As an additional example, we can assume that a population has two stages:

* Corresponding author.
*E-mail address:* keshab_bg@yahoo.in (B. Ghosh).

https://doi.org/10.1016/j.chaos.2019.03.002
0960-0779/

immature and mature, and the newborns get matured in $\tau$ units of time. Under such a consideration, the current growth of the adult population depends upon the number of newborns which were present at time $(t-\tau)$. Thus, ecologists have developed mathematical models of predator-prey system incorporating time delay. Although, non-linear functional responses cause non-equilibrium dynamics following oscillations and chaos, time delay can also lead to instability in predator-prey systems. Some of the pioneer works based on single-species model incorporating time delay are discussed by Hutchinson [18], Nicholson [40], Beddington and May [2] and Freedman and Gopalsamy [7] in the context of theoretical ecology. These contributions discuss about the global stability of the steady state, existence of Hopf-bifurcation and length of delay for which stability is ensured. However, time delay plays an important role in modeling dynamics of multi-species interactions [4,30], eco-epidemiology and epidemiology [52,55,56].

The delay induced dynamics in predator-prey systems and tritrophic food chains are studied by many researchers. Three types of time delays are mainly incorporated in analyzing predator-prey systems: (a) time delay is involved in prey specific growth function, (b) delay is included in predation response function and (c) delay is incorporated in the interacting function of the predator equation. Ho and Ou [17] considered Lotka–Volterra type (logistic prey growth in absence of predator and Holling type I functional response) predator-prey system with time delay in prey growth. They have proved the existence of stability switching due to time delay. Stage-structure predator-prey model can also experience oscillation due to maturation delay [14]. Li and Takeuchi [31] have proved the global stability result of the coexisting equilibrium in a delayed predator-prey system with Beddington–DeAngelis functional response. A detailed algorithm for the direction of Hopf-bifurcation is established through the study of a delayed Holling–Tanner predator-prey system by Zhang [57]. Shu et al. [47] have shown that three types of bistability are possible in a delayed intraguild predation model: one is node-node bistability; another one is node-cycle bistability and the final one is cycle-cycle bistability. Shi and Yu [46] analyzed Hopf-bifurcation in a two zooplanktons and one-phytoplankton model with two delays. A two-prey and one predator system with distinct time delays in the logistic prey growth for both the prey populations was investigated by Kundu and Maitra [26], and have determined critical value of delay parameters for which the system can be destabilized.

A large number of rich literatures are also available to address harvesting impacts in delayed population dynamics models. A delayed Lotka–Volterra type predator-prey model under proportional harvesting was investigated by Toaha et al. [49]. They have observed the occurrence of stability switching and determined range of effort for which stability got changed. On the other hand, Toaha and Hassan [48] proved that there exists a parametric condition under which delay does not cause instability in Lotka–Volterra type system with constant rate of harvesting for both the species. However, delay causes stability switching as well under different parameter condition. Xia et al. [54] applied non-trivial mathematical theory to study the direction of Hopf-bifurcation in a delayed predator-prey system under constant rate harvesting. A ratio-dependent predator-prey system under time delay in predation process and harvesting the predator was analyzed by Misra and Dubey [39]. They have mentioned that Hopf-bifurcation is observed due to time delay. Roy et al. [44] also studied a harvested predator-prey model under time delay and Beddington–Deangelis functional response. Very recently, Liu and Jiang [34] have used effective mathematical and simulation tools in a delayed predator-prey system under Michaelis–Menten type harvesting of prey species and analyzed the delay induced stability switching. A predator-prey type model was considered under harvesting to derive Hopf-bifurcation phenomenon due to multiple delays by Juneja et al. [19].

Of course, the above articles developed the models under time delay and harvesting. However, we feel that the explicit impacts of harvesting have not been examined properly by the above contributions (including [32,33,53]). These notable contributions mainly analyzed the dynamics under time delay and checked whether time delay causes instability or stability switching. Hence, the analysis of the harvested system is qualitatively similar to the models without harvesting. There are very few articles which partially investigated the explicit effects of harvesting following numerical simulations. Martin and Ruan [35] are the first who presented the impact of harvesting explicitly in three distinct predator-prey models. In fact, their analytical theory only described the delay induced stability behavior of the models. However, they explained the impact of harvesting using numerical simulation as the model becomes very complex to solve analytically due to constant harvesting rate. They observed numerically that, when the delay was incorporated in logistic term in Gause-type predator-prey model, prey harvesting stabilized the system which was at unstable mode. Similarly, Kar and Pahari [24] studied RM model with time delay in logistic growth and concluded the same outcome like Martin and Ruan [35] when proportional harvesting strategy is applied to prey population. They conducted another numerical simulation to show that predator harvesting has a destabilizing effect in the system dynamics. A Leslie–Grower predator-prey system with time delay in functional response was studied by Kar and Ghorai [21] and found through simulation that harvesting of either prey or predator can stabilize a pre-harvested unstable system. Meng et al. [38] have numerically established that either prey or predator harvesting stabilized a predator-prey system incorporating Beddington–DeAngelis functional response which was at unstable mode due to delay before harvesting.

Our motivations for this research are as follows: the above discussion clearly claims that there is a need to conduct more research in this direction. Martin and Ruan [35] have only focused on studying the impact when prey is harvested. Therefore, we should pay attention to analyze predator harvesting, as predator harvesting is safe for the persistence of ecosystem. Moreover, predatory fish is harvested at higher rate for commercial purposes. Martin and Ruan [35], Kar and Ghorai [21] and Meng et al. [38] have only shown numerically that unstable dynamics can be stabilized due to harvesting. We would like to know whether any other distinct dynamics is possible when predator-prey model takes different form. Moreover, we examine if a stable system always stay stable due to harvesting in a delayed system. In addition, Ghosh et al. [10] demonstrated that harvesting the prey or predator or both species can stabilize a non-delayed RM predator-prey system. Thus, it seems that the harvesting results in delayed and non-delayed systems are qualitatively same. We verify if the above statement does hold in ecological system. Also Kar and Pahari [24], Kar [20] and Martin and Ruan [35] have mentioned that there is a situation for which the coexisting equilibrium does not change stability due to delay. We would like to reanalyze this result. We would also address here the implementation of MSY policy in delayed system. We acknowledge Martin and Ruan [35] for showing the research direction of implementing MSY policy in predator-prey models. To the best of our knowledge, it is not addressed by anyone. By and large, our motivations for this investigation are relevant in these aspects.

Most of the predator-prey systems are analyzed by varying the time delay as control parameters to describe several dynamics. However, it may not be very much relevant to vary as time delay is an inherent factor in a system. In particular, when harvesting is implemented in a fishery system, instead of varying time delay, we have much freedom to regulate fishing effort since it is an

ecological fact that time delay factor changes in very slow time scale. Thus, in our analysis we assume that time delay is invariant in a system and fishing effort varies.

The paper addresses the following major issues:

(i) whether LV type model experiences only stability switching due to time delay.
(ii) whether there is any parametric restriction for which time delay does not induces instability in RM model.
(iii) whether harvesting can locally stabilize (respectively, destabilize) the system when the unharvested system is at unstable dynamics (respectively, stable steady state mode).
(iv) whether a stable steady state can always be obtained when predator is harvested towards MSY level.

The paper is organized as follows. Section 2 is devoted to description of dynamics of Lotka–Volterra type predator-prey model incorporating time delay. The impacts of harvesting in the model are extensively studied. The existence of MSY at stable steady state is also discussed. Section 3 deals with delay induced stability and the harvesting effects in Rosenzweig–MacArthur predator-prey system. The last section discusses our main results and compares them with the existing literatures. Many new results are established and some of the existing results are improved. This section ends with future perspectives of research in this field.

## 2. Lotka–Volterra type model

To response the issues raised in the Introduction Section, we first consider LV type predator-prey model. The dynamics of the unharvested LV type system is analyzed when time delay is the control parameter. Then, the distinct dynamical behaviors are explained by varying harvesting effort, keeping time delay fixed.

### 2.1. Dynamics of delayed LV type model

We consider the Lotka–Volterra type predator-prey model given by the following coupled system:

$$\dot{x} = rx\left(1 - \frac{x(t-\tau)}{K}\right) - \alpha xy,$$
$$\dot{y} = \beta xy - my. \tag{1}$$

Here $x(t)$ and $y(t)$ are the prey and predator population, respectively, at time $t$, $r$ is the intrinsic growth rate of the prey, $K$ is the carrying capacity of the prey population in the absence of the predator, $\alpha$ the rate of prey consumption by the predator, $\beta$ the conversion rate of prey consumed into the predator growth rate and $m$ is the mortality rate of the predator.

The equilibrium points of the model are

$$(0,0),\ (K,0) \text{ and } (x^*, y^*) = \left(\frac{m}{\beta}, \frac{r(K\beta - m)}{\alpha\beta K}\right),$$

where $K > \frac{m}{\beta}$ for existence of interior equilibrium.

To check for the local stability, we use the transformation $u = x - x^*$, $v = y - y^*$ for obtaining the linearized system corresponding to (1) as,

$$u^* = -\frac{r}{K}x^*u(t-\tau) - \alpha x^*v,$$
$$v^* = \beta y^*u. \tag{2}$$

The characteristic equation associated with the above linearized system is given by,

$$\lambda^2 + \frac{r}{K}x^*\lambda e^{-\lambda\tau} + \alpha\beta x^*y^* = 0$$

$$\text{i.e. } \lambda^2 + P\lambda e^{-\lambda\tau} + Q = 0, \tag{3}$$

where $P = \frac{r}{K}x^*$ and $Q = \alpha\beta x^*y^*$. We first check for the stability when $\tau = 0$. When $\tau = 0$, the roots are given by,

$$\lambda = \frac{\frac{-r}{K}x^* \pm \sqrt{(\frac{r}{K}x^*)^2 - 4\alpha\beta x^*y^*}}{2}.$$

Since both the roots have negative real part, the interior steady state is locally asymptotically stable at $\tau = 0$. We now examine the stability behavior of the system with increase in $\tau$.

Let us check for the existence of a positive $\omega$ such that $\lambda = i\omega$.

When $\lambda = i\omega$, the characteristics Eq. (3) after separating the real and imaginary parts, can be written as,

$$-\omega^2 + \omega\frac{r}{K}x^*\sin(\omega\tau) + \alpha\beta x^*y^* = 0 \tag{4a}$$

$$\frac{r}{K}x^*\omega\cos(\omega\tau) = 0. \tag{4b}$$

From the Eq. (4b), we get

$$\omega\tau = \begin{cases} \frac{\pi}{2} + 2n\pi = \theta_1 \\ \frac{3\pi}{2} + 2n\pi = \theta_2, \quad n = 0, 1, 2, \ldots \end{cases}$$

If $\omega\tau = \frac{\pi}{2} + 2n\pi$, then Eq. (4a) is reduced to

$$\omega^2 - \omega\frac{r}{K}x^* - \alpha\beta x^*y^* = 0.$$

The above equation has only one positive root for $\omega$ which is given by,

$$\omega = \omega_+ = \frac{P + \sqrt{P^2 + 4Q}}{2}.$$

Hence, we can obtain

$$\tau = \tau_n^+ = \frac{\pi}{2\omega_+} + \frac{2n\pi}{\omega_+}, \quad n = 0, 1, 2, \ldots$$

Similarly, when $\omega\tau = \frac{3\pi}{2} + 2n\pi$, the corresponding equation

$$\omega^2 + \omega\frac{r}{K}x^* - \alpha\beta x^*y^* = 0$$

also produces a unique positive value $\omega_-$ given as,

$$\omega_- = \frac{-P + \sqrt{P^2 + 4Q}}{2}.$$

Hence, we can compute

$$\tau = \tau_n^- = \frac{3\pi}{2\omega_-} + \frac{2n\pi}{\omega_-}, \quad n = 0, 1, 2, \ldots$$

The above analysis demonstrates that at least one pair of eigenvalues has zero real part at $\tau = \tau_n^{\pm}$. We now verify whether the real part of the eigenvalues changes their sign when $\tau$ crosses $\tau_n^{\pm}$. In order to know the rate of change of real part of the eigenvalues with respect to $\tau$ at $\tau_n^{\pm}$, we take into account the well known transversality condition to obtain,

$$\left(\frac{d\lambda}{d\tau}\right)^{-1} = \frac{-\lambda^2 + Q}{\lambda^2(\lambda^2 + Q)} - \frac{\tau}{\lambda}.$$

We know that $\tau = \tau_n^{\pm}$ corresponds $\lambda = \pm i\omega$. Hence,

$$\left(\frac{d\lambda}{d\tau}\right)^{-1}\Big|_{\tau=\tau_n^{\pm}} = \frac{\omega^2+Q}{-\omega^2(-\omega^2+Q)} - \frac{\tau}{i\omega}$$

$$\Rightarrow \text{sign}\left(Re\left(\frac{d\lambda}{d\tau}\right)\right)^{-1}\Big|_{\tau=\tau_n^{\pm}} = \text{sign}(\omega^4 - Q^2).$$

Squaring and adding (4a) and (4b), we have,

$$2\omega^4 - P^2\omega^2 - 2Q\omega^2 + Q^2 - \omega^4 = 0.$$

Hence,

$$\text{sign}\left(\frac{d(Re\lambda)}{d\tau}\right)^{-1}\Big|_{\tau=\tau_n^{\pm}} = \text{sign}(2\omega^2 - (P^2+2Q)).$$

Finally,

$$\frac{dRe\lambda}{d\tau}\Big|_{\tau_n^+} > 0 \ \ \& \ \ \frac{dRe\lambda}{d\tau}\Big|_{\tau_n^-} < 0.$$

The above conditions reveal that if real part of any eigenvalue is zero at $\tau = \tau_n^+$ (respectively $\tau = \tau_n^-$), real part of the eigenvalue becomes positive (respectively negative) for increasing $\tau$ near $\tau_n^+$ (respectively $\tau_n^-$). Consequently, Hopf-bifurcations take place at $\tau = \tau_n^{\pm}$ for the interior equilibrium $(x^*, y^*)$.

We are now interested to know the number of eigenvalues crossing the imaginary $\lambda$ -axis. The following lemma will verify the same.

**Lemma 2.1.** *The roots of the function $F(\lambda, \tau) = \lambda^2 + a\lambda e^{-\lambda\tau} + c$, where $a$, $c > 0$, are simple on the imaginary axis [5].*

**Proof.** Let us suppose the function $F(\lambda, \tau)$ has a root $i\omega$ on the imaginary axis and it is not simple. Then $\frac{\partial F}{\partial \lambda}|_{\lambda=i\omega} = 0$ i.e. $2\lambda + (1 - \tau\lambda)be^{-\lambda\tau} = 0$ for any $\lambda = i\omega$. Substituting the value of $\lambda = i\omega$ and the value of $e^{-\lambda\tau}$ from $F(\lambda, \tau) = 0$, we get, $\omega^2 + c = 0$, which is impossible. Hence, the eigenvalues $i\omega$ and $-i\omega$ of our linearized system are simple.

This lemma also states that at each $\tau = \tau_n^+$ (or $\tau = \tau_n^-$) corresponding to our linearized system only a pair of eigenvalues cross the imaginary axis. □

**Remark.** Since $\omega_+ > \omega_-$,

$$\tau_{n+1}^+ - \tau_n^+ = \frac{2\pi}{\omega_+} < \frac{2\pi}{\omega_-} = \tau_{n+1}^- - \tau_n^-,$$

for $n = 0, 1, 2, \ldots$.

We now establish the stability theory due to increasing delay as follows.

**Theorem 2.1.** *If $\tau_0^+ < \tau_1^+ < \tau_0^-$, the system maintains stable behavior for $\tau \in [0, \tau_0^+)$, experience a Hopf-bifurcation at $\tau = \tau_0^+$ and finally becomes unstable for $\tau > \tau_0^+$.*

**Proof.** We assume that $\tau_0^+ < \tau_1^+ < \tau_0^-$. The system is stable for $\tau = 0$ as the real part of both the roots associated with the characteristic equation are negative. When delay is increased, then $\lambda = i\omega_+$ will be a simple eigenvalue of the characteristic equation at $\tau = \tau_0^+$ (see Lemma 2.1). Since eigenvalues occur in complex conjugate, there exists exactly one pair of eigenvalues $\lambda = \pm i\omega_+$ at $\tau = \tau_0^+$.

The positivity of the associated transversality condition at $\tau = \tau_0^+$ suggests that the aforementioned pair of eigenvalues cross the imaginary axis and contain positive real part when delay increases and close to $\tau_0^+$. Hence the system becomes unstable.

Again when the delay $\tau$ reaches at $\tau_1^+$, again another pair of eigenvalues take the form $\lambda = i\omega_+$. Then the transversality condition at $\tau = \tau_1^+$ tells us that the said pair cross the imaginary axis. Therefore, there exists two pair of eigenvalues with real part positive when $\tau > \tau_1^+$. Hence the system becomes unstable.

Using the similar arguments, a pair of eigenvalues of the form $\lambda = \pm i\omega_-$ occurs at $\tau = \tau_0^-$. Then the transversality condition causes the said pair eigenvalues to cross the imaginary axis and obtain negative real part. Thus, pair of eigenvalues still stay with positive real part when $\tau$ increases through $\tau_1^+$ and instability still persists.

Since at each $\tau = \tau_n^+$ or $\tau_n^-$, only one pair of eigenvalues cross the imaginary axis and there is no possibility of the occurrence of two consecutive $\tau_n^-$ (see Remark 2.1), the instability persists forever with $\tau > \tau_0^+$. □

**Example 2.1.** We verify the existence of such dynamical behavior by considering $r = 0.8$, $K = 20$, $\alpha = 0.4$, $\beta = 0.1$, $m = 0.9$ in model (1). The interior equilibrium associated with the system is (9, 1.1). Here the values of $\tau_0^+ = 1.8823$, $\tau_1^+ = 9.4113$ and $\tau_0^- = 9.9308$. It is observed that the system is stable for $\tau \in [0, 1.8823]$ and for all $\tau > 1.8823$ it is unstable.

**Theorem 2.2.** *If $0 < \tau_0^+ < \tau_0^- < \tau_1^+ < \tau_1^- < \ldots < \tau_k^+ < \tau_{k+1}^+ < \tau_k^- < \ldots$ for some positive integer $k$, then $k$ switches from stability to instability to stability occurs and eventually for $\tau > \tau_k^+$ the system becomes unstable. Further at $\tau = \tau_n^{\pm}$, the system experiences Hopf-bifurcation.*

**Proof.** Let us first consider the inequality $\tau_0^+ < \tau_0^- < \tau_1^+$. Here, $\tau_0^+, \tau_0^-, \tau_1^+$ are the time delays for which Hopf-bifurcation occurs. It is already shown that the system is stable at $\tau = 0$ due to presence of negative roots of the characteristic Eq. (3). An increase in $\tau$ leads to a pair of purely imaginary roots $(\pm i\omega_+)$ of (3) at $\tau = \tau_0^+$. The transversality condition at $\tau_0^+$ indicates the appearance of eigenvalues with positive real part for the said pair when delay increases through $\tau_0^+$. Thus, the system will no longer be in stable state. Further increase in the value of $\tau$ will again lead to a purely imaginary root at $\tau_0^-$. But the transversality condition at $\tau_0^-$ indicates that the two eigenvalues with positive real part, which possess purely complex values $(\pm i\omega_-)$ at $\tau_0^-$, eventually has negative real part and increase in $\tau$ through $\tau_0^-$, which results in stability of the system. Hence, a stability switching from stable to unstable to stable takes place at the interior equilibria of the system (1) with increase in $\tau$.

Similarly, for all other $\tau \le \tau_k^-$, the switching of stability will be continued followed by the earlier discussion till $\tau < \tau_k^+$. Therefore, we can observe the occurrence of $k$ number of stability switching. Once the delay satisfy $\tau_k^+ < \tau_{k+1}^+ < \tau_k^-$, the arguments in Theorem 2.1 reveals that the system becomes unstable for all $\tau > \tau_k^+$. □

**Corollary 2.1.** *The number of switches from stability to instability and back to stability which may take place in the system (1) can be determined by the smallest value of $k$ which satisfies the equation $4(k+1)P > \sqrt{P^2 + 4Q}$. Further as in the case of Theorem 2.1, the absence of stability switching will make the system (1) satisfy the equation $4P > \sqrt{P^2 + 4Q}$.*

**Example 2.2.** Let us consider the parameters as: $r = 1$, $K = 180$, $m = 1$, $\alpha = 0.3$ and $\beta = 0.1$ in model (1). Then the coexisting steady state $(x^*, y^*) = (10, 3.1481)$ of the non-delayed model is asymptotically stable. Now by increasing the values of $\tau$, the system experiences 8 switching from stability to instability and back to stability. However, there exists $\tau_8^+$, such that the system is unstable for all $\tau > \tau_8^+$. The values of different $\tau_n^{\pm}$'s are listed.

$\tau_0^+ \approx 1.5708$ $\tau_0^- \approx 4.9896$
$\tau_1^+ \approx 7.8540$ $\tau_1^- \approx 11.6424$
$\tau_2^+ \approx 14.1372$ $\tau_2^- \approx 18.2952$
$\tau_3^+ \approx 20.4204$ $\tau_3^- \approx 24.9479$
$\tau_4^+ \approx 26.7035$ $\tau_4^- \approx 31.6007$
$\tau_5^+ \approx 32.9867$ $\tau_5^- \approx 38.2535$
$\tau_6^+ \approx 39.2699$ $\tau_6^- \approx 44.9063$
$\tau_7^+ \approx 45.5531$ $\tau_7^- \approx 51.5591$
$\tau_8^+ \approx 51.8363$ $\tau_8^- \approx 58.2119$
$\tau_9^+ \approx 58.1195$

As we have discussed earlier, the system (1) is stable for all $\tau \in (0, \tau_0^+) \cup (\tau_0^-, \tau_1^+) \cup (\tau_1^-, \tau_2^+) \cup (\tau_2^-, \tau_3^+) \cup (\tau_3^-, \tau_4^+) \cup (\tau_4^-, \tau_5^+) \cup (\tau_5^-, \tau_6^+) \cup (\tau_6^-, \tau_7^+) \cup (\tau_7^-, \tau_8^+)$ and is unstable for all $\tau \in (\tau_0^+, \tau_0^-) \cup (\tau_1^+, \tau_1^-) \cup (\tau_2^+, \tau_2^-) \cup (\tau_3^+, \tau_3^-) \cup (\tau_4^+, \tau_4^-) \cup (\tau_5^+, \tau_5^-) \cup (\tau_6^+, \tau_6^-) \cup (\tau_7^+, \tau_7^-) \cup (\tau_8^+, \infty)$. At $\tau = \tau_n^{\pm}$, Hopf-bifurcation occurs.

### 2.2. Harvesting results in LV type model

Time delay in an ecological system may vary slowly or more prominently due to seasonal changes, human induced perturbations or some inherent activity of the concerned species. A slow change in time delay may be considered as constant. In this paper, we assume that delay in a specific system is not changing in time. In fact, ecological parameters (such as time delay) are not much affected from outside in peaceful environment (normal circumstances), but we can control the harvesting effort as per our convenient. Therefore, considering the fixed time delay in the system, we would like to investigate the dynamics under harvesting. The predator-prey system can be in a specific dynamics mode (stable or non-equilibrium) for a fixed time delay. We now successively study on how the unexploited dynamics can be changed when prey and predator are harvested individually.

#### 2.2.1. Prey harvesting

We consider the Lotka–Volterra type predator-prey model with time delay $\tau$ in the prey specific growth rate under prey harvesting as:

$$\begin{aligned} \dot{x} &= rx\left(1 - \frac{x(t-\tau)}{K}\right) - \alpha xy - E_1 x, \\ \dot{y} &= \beta xy - my, \end{aligned} \tag{5}$$

where $E_1$ is the effort of harvesting of prey population.

The equilibrium points of the model are

$$(0,\ 0),\ \left(\frac{K(r-E_1)}{r},\ 0\right) \quad \text{and}$$

$$\left(\frac{m}{\beta}, \left(\frac{r(K\beta - m)}{K\alpha\beta} - \frac{E_1}{\alpha}\right)\right).$$

The effort of harvesting for the existence of positive equilibrium must satisfy

$$0 < E_1 < \frac{r(K\beta - m)}{K\beta}. \tag{6}$$

Linearizing the system near positive interior equilibrium, we get the characteristic equation,

$$\lambda^2 + \lambda e^{-\lambda\tau}\left(\frac{rm}{K\beta}\right) + m\left(\frac{r(K\beta - m)}{K\beta} - E_1\right) = 0. \tag{7}$$

As in the previous section, we observe that, when $\tau = 0$, the system is stable. Let us assume, there exist value of $\lambda$, $\lambda = i\omega$ ($\omega > 0$), such that change in stability takes place from stable to unstable and vice versa.

Similarly, as in the previous section, we substitute the value of $\lambda = i\omega$ in (7) to get the values of $\omega$ as,

$$\omega_{\pm}(E_1) = \frac{\pm P_1 + \sqrt{P_1^2 + 4Q_1}}{2} \tag{8}$$

where $P_1 = \frac{rm}{K\beta}$ and $Q_1 = m\left(\frac{r(K\beta - m)}{K\beta} - E_1\right)$.

And the values of $\tau$ corresponding to the above $\omega_+$ and $\omega_-$ are given as,

$$\tau_n^+(E_1) = \frac{\pi}{2\omega_+} + \frac{2n\pi}{\omega_+} \tag{9}$$

and

$$\tau_n^-(E_1) = \frac{3\pi}{2\omega_-} + \frac{2n\pi}{\omega_-}. \tag{10}$$

where $n = 0, 1, \ldots$

Here, unlike the previous section, based on the different efforts of harvesting $E_1$, we get different set of values of $\omega_{\pm}(E_1)$ and $\tau_n^{\pm}(E_1)$. Accordingly, we get the below lemma and theorems.

**Remark.** Here $\tau_n^+(0)$ is the time delay when there is no harvesting. For simplicity we sometimes use $\tau_n^+$ instead of $\tau_n^+(0)$.

**Lemma 2.2.** *In system (5), the values of $\tau_n^{\pm}(E_1)$ increases with increase in the harvesting effort $E_1$, i.e. $\tau_n^{\pm}(E_1)$ is an increasing function of $E_1$.*

**Proof.** Clearly it can be seen from (8), that with increase in $E_1$ keeping all the other parameters fixed, $Q_1$ decreases leading to decrease in $\omega_{\pm}(E_1)$ and increase in $\tau_n^{\pm}(E_1)$. Thus $\tau_n^{\pm}(E_1)$ is an increasing function of $E_1$. □

**Theorem 2.3.** *If the pre-harvested system (1) incorporates time delay $\mathcal{T}$ in the range $(0, \tau_0^+(0))$, prey harvesting cannot change the stability nature of the system.*

**Proof.** If time delay $\mathcal{T} \in (0, \tau_0^+(0))$, it results the stability in the unharvested system. Now it can be seen from Lemma 2.2 that $\tau_0^+(E_1)$ will increase with increasing effort $E_1$. Thus $\mathcal{T} \in (0, \tau_0^+(0)) \subseteq (0, \tau_0^+(E_1))\ \forall\ E_1$. Hence the stable state of the unharvested system will persist. □

Now we consider the ecological parameters satisfying the condition $\tau_0^+(0) < \tau_1^+(0) < \tau_0^-(0)$ (see Theorem 2.1). Then the system does not exhibit any stability switching. Thus, a change in delay can cause instability in the pre-harvested system. From the above discussion, it is clear that harvesting the prey species does not change the stability when $\mathcal{T} \in (0, \tau_0^+(0))$. We would like to investigate the stability due to harvesting when delay $\mathcal{T} > \tau_0^+(0)$. The related results are presented in the following theorem.

**Theorem 2.4.** *Under the above parameter conditions, the following two cases arise:*

(i) *If $\mathcal{T} \in (\tau_0^+(0), \tau_{\max})$, the instability in the system can be removed by a suitable effort and further increase of the effort does not alter the stability of the system. Here $\tau_{\max} = \lim_{E_1 \to E^*} \tau_0^+(E_1)$ and $E^* = \frac{r(K\beta - m)}{K\beta}$.*

(ii) *If $\mathcal{T} > \tau_{\max}$, harvesting cannot stabilize the system.*

**Proof.**

(i) When the prey population is harvested, the system is stable for all $(E_1, \mathcal{T}) \in (0, E^*) \times (0, \tau_0^+(E_1))$ and unstable for $(E_1, \mathcal{T}) \in (0, E^*) \times (\tau_0^+(E_1), \infty)$. Let $\mathcal{T} \in (\tau_0^+(0), \tau_{\max})$. Since $\tau_0^+(E_1)$ is an increasing function of effort (see Lemma 2.2), the coordinate $(E_1, \mathcal{T})$, which lies in $(0, E_1) \times (\tau_0^+(E_1), \tau_{\max})$ for smaller effort, can be shifted to the region $(0, E^*) \times (0, \tau_0^+(E_1))$ beyond a critical effort. Hence the system achieves the stability.

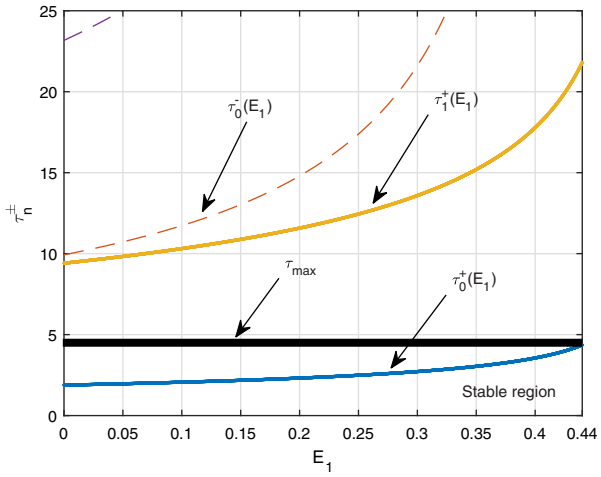


**Fig. 1.** The curves $\tau = \tau_n^{\pm}(E_1)$ are increasing function of effort. The stability region in the $E_1\tau$-plane under harvesting is shown.

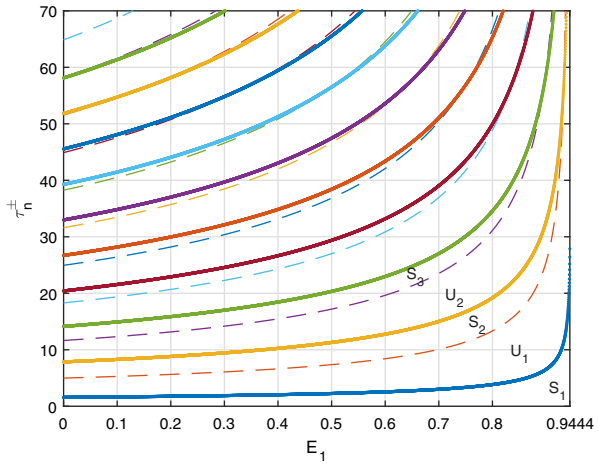


**Fig. 2.** The solid curves $\tau = \tau_n^+(E_1)$ and dashed curves $\tau = \tau_n^-(E_1)$ traps various regions of stabilities $S_n$ and instabilities $U_n$ in between them.

(ii) Now for $\mathcal{T} > \tau_{\max}$, any coordinate $(E_1, \mathcal{T})$ cannot be shifted into the region $(0, E^*) \times (0, \tau_0^+(E_1))$. Hence the system will remain unstable for any harvesting effort. □

We will explain the above theorem with numerical simulations. Consider the parameters as given in Example 2.1. For coexistence of both the populations, effort must lie in the range (0, 0.44). The dashed curves are plotted for $\tau = \tau_n^-(E_1)$ $(n = 0, 1)$ (see Fig. 1). The horizontal solid black curve represent $\tau = \tau_{\max}$ and the remaining solid curves represents $\tau = \tau_n^+(E_1)$ $(n = 0, 1)$. The region enclosed by the $E_1$-axis and the $\tau = \tau_0^+(E_1)$ curve is the region of stability and the whole region afterwards is the region of instability. It can be seen that for $\mathcal{T}$ lying between $(0, \tau_0^+(0))$, the coordinate $(E_1, \mathcal{T})$ stays in the region of stability for increasing $E_1$ as stated in Theorem 2.4(a). Here $\tau_{\max} = 4$. It can be seen that for $\mathcal{T} \in (\tau_0^+(0), \tau_{\max})$, the coordinate $(E_1, \mathcal{T})$ will stay in the unstable region bounded by $\tau = \tau_{\max}$ and $\tau = \tau_0^+(E_1)$ for smaller effort. However, the coordinate enters into the stability region for increasing effort as stated in Theorem 2.4(b) and for $\mathcal{T} > \tau_{\max}$, the point $(E_1, \mathcal{T})$ remains in the unstable region for any effort as stated in Theorem 2.4 (c).

The above analysis reveals that the harvested system does not change stability behavior if the unharvested system is stable. On the other hand, if the time delay is larger $(\mathcal{T} > \tau_{\max})$, instability behavior can not be altered by prey harvesting. However, for a moderate length time delay $(\tau_0^+(0) < \mathcal{T} < \tau_{\max})$, the system can be stabilized beyond some critical effort.

Now we are going to investigate the harvesting impact when the unharvested system exhibits delay induced stability switching. We consider the ecological parameters given in Example 2.2 for the system (5). It is observed that the unharvested system experience eight stability switching from stable to unstable and back to stable due to delay. However, after the eight stability switches, further increase in delay will result in instability in the system as can be seen in Example 2.2. The range of $E_1$ for existence of positive equilibrium is (0, 0.9444). Likewise the previous analysis, we plot different curves $\tau = \tau_n^{\pm}(E_1)$ as shown in Fig. 2.

The solid curves and dashed curves in the Fig. 2 represents $\tau = \tau_n^+(E_1)$ and $\tau = \tau_n^-(E_1)$, $(n = 0, 1, 2, ...)$ respectively. The region between the $E_1$-axis and the first solid curve is the region of stability. The region enclosed by any solid curve and succeeding dashed curve is the region of instability. The region enclosed by any dashed curve and succeeding solid curve are the region of stability until intersection takes place between these two curves for increasing effort. After the intersection, there will be simultaneous appearance of two solid curves. These consecutive appearance of two solid curves results in instability regions between the curves as well as the regions above the curves, for that particular range of $E_1$. Let us denote the region bounded by the $E_1$-axis and the $\tau = \tau_0^+(E_1)$ as $S_1$, the region bounded by $\tau = \tau_n^+(E_1)$ and $\tau = \tau_n^-(E_1)$ as $U_{n+1}$, and the region bounded by $\tau = \tau_n^-(E_1)$ and $\tau = \tau_{n+1}^+(E_1)$ as $S_{n+2}$ $(n = 0, 1, ...)$. It can be observed that the regions $S_1, S_2, S_3$ are the region of stability and the regions $U_1, U_2$ are the region of instability until the two $\tau = \tau_n^+(E_1)$ and $\tau = \tau_{n+1}^+(E_1)$ appear one after another which results in appearance of instability regions.

The following stability behavior can be observed due to harvesting (see Fig. 2) once the time delay is invariant in the system (5).

(i) For $\mathcal{T} \in (0, \tau_0^+(0)) = (0, 1.5708)$, the coordinate $(E_1, \mathcal{T})$ remains in region $S_1$ for any effort of harvesting. Thus, the system is stable throughout.

(ii) For $\mathcal{T} \in (\tau_0^+(0), \tau_0^-(0)) = (1.5708, 4.9896)$, the coordinate $(E_1, \mathcal{T})$ stays in region $U_1$ until the effort of harvesting is large enough to push it from region $U_1$ to $S_1$. Thus, for larger effort of harvesting, the instability can be removed and both the population will coexist at the steady state.

(iii) For $\mathcal{T} \in (\tau_0^-(0), \tau_1^+(0)) = (4.9896, 7.8540)$, the coordinate $(E_1, \mathcal{T})$ shifts from region $S_2$ to $U_1$ and then to $S_1$ with increasing harvesting strength. In fact the coordinate enters into the region $S_1$ when effort is sufficiently close to the critical effort $E^*$. Such an harvesting effort leads to a steady stable state with smaller predator density. Shifting of the regions indicates that the stable unharvested system can be destabilized by harvesting effort, but the system regains its stability for further increasing effort. Hence, one stability switching occurs for increasing effort.

(iv) For $\mathcal{T} \in (\tau_1^+(0), \tau_1^-(0)) = (7.8540, 11.6424)$, the coordinate $(E_1, \mathcal{T})$ shifts from region $U_2$ to $S_2$ and then to $U_1$ with increasing harvesting effort. Shifting of the regions indicates that the instability in the unharvested system can be made stable with increasing effort, but further increase can again lead to instability in the system. Hence, an instability switching occurs.

(v) For $\mathcal{T} \in (\tau_1^-(0), \tau_2^+(0)) = (11.6424, 14.1372)$, there is successive shifting of the coordinate $(E_1, \mathcal{T})$ through the regions $S_3$, $U_2$, $S_2$ and $U_1$ with increasing harvesting strength.

(vi) For $\mathcal{T} > \tau_{\max}^+(E')$, the system remains unstable for all effort of harvesting, where $\tau_{\max}^+(E')$ is the maximum of all the $\tau_k^+(E')$ such that $k \leq 8$ is the number of switching of the system for each $E_1$. We note that it is the case which was observed in the Theorem 2.4(b).

*2.2.2. Predator harvesting*

In this section, we deal with the Lotka–Volterra type model under predator harvesting. The model under predator harvesting reads as:

$$\dot{x} = rx\left(1 - \frac{x(t-\tau)}{K}\right) - \alpha xy,$$

$$\dot{y} = \beta xy - my - E_2 y, \tag{11}$$

where $E_2$ is the effort of harvesting of predator population.

The steady states of the model are

$$(0,0),\ (K,0),\ \left(\frac{m+E_2}{\beta}, r\left(\frac{K\beta - m}{K\alpha\beta} - \frac{E_2}{K\alpha\beta}\right)\right).$$

The effort of harvesting for the co-existence of positive steady state must satisfy

$$0 < E_2 < K\beta - m. \tag{12}$$

Linearizing the system near positive interior equilibrium, we obtain the following characteristics equation,

$$\lambda^2 + \lambda e^{-\lambda\tau}\left(\frac{r(m+E_2)}{K\beta}\right) + \frac{r}{K\beta}(m+E_2)\{K\beta - (m+E_2)\} = 0. \tag{13}$$

As before, we compute the eigenvalues for the occurrence of Hopf-bifurcation. The eigenvalues $i\omega_\pm(E_2)$, where Hopf-bifurcation occurs, are determined as:

$$\omega_\pm(E_2) = \frac{\pm P_2 + \sqrt{P_2^2 + 4Q_2}}{2} \tag{14}$$

where $P_2 = \frac{r(m+E_2)}{K\beta}$ and $Q_2 = \frac{r}{K\beta}(m+E_2)\{K\beta - (m+E_2)\}$.

And the values of $\tau$ corresponding to $\omega_+$ and $\omega_-$ are given as,

$$\tau_n^+(E_2) = \frac{\pi}{2\omega_+} + \frac{2n\pi}{\omega_+} \tag{15}$$

and

$$\tau_n^-(E_2) = \frac{3\pi}{2\omega_-} + \frac{2n\pi}{\omega_-}. \tag{16}$$

where $n = 0, 1, \ldots$

Here, we attain different set of values of $\omega_\pm(E_2)$ and $\tau_n^\pm(E_2)$ based on the different efforts of harvesting $E_2$. We divide the analysis for predator harvesting into two different cases.

***Case I: When the unharvested system does not experience delay induced stability switching***

In this case, we assume that the unharvested system only exhibits delay induced instability, in the sense that, the system does not gain the stability back due to increasing delay once the system looses its stability. In other words, there exists $\tau_0^+$, such that, the system is stable for $\tau < \tau_0^+$ and unstable for $\tau > \tau_0^+$ with a Hopf-bifurcation at $\tau = \tau_0^+$. We show that the curve $\tau = \tau_0^+(E_2)$ takes two different forms; one is decreasing and the other is unimodal with a minimum, in the co-existing effort range. Hence, distinct dynamical behavior under harvesting can be described as follows.

We consider the parameters to be: $r = 1,\ K = 20,\ m = 0.1,\ \alpha = 0.1,\ \beta = 0.01$, such that it satisfies the condition $\tau_0^+(0) < \tau_1^+(0) < \tau_0^-(0)$. The populations will persist for effort of harvesting lying in the range (0, 0.1). The solid blue curve represent $\tau = \tau_0^+(E_2)$ which is decreasing in effort (see Fig. 3). The two black curves represent $\tau = \tau_{\max}$ and $\tau = \tau_0^+(0)$, where $\tau_{\max} = \lim_{E_2 \to 0.1} \tau_0^+(E_2)$. The region enclosed by the $E_2$-axis and $\tau = \tau_0^+(E_2)$ is the region of stability and the whole region afterwards is the region of instability. The following stability behavior were observed based on the range of $\mathcal{T}$ value.

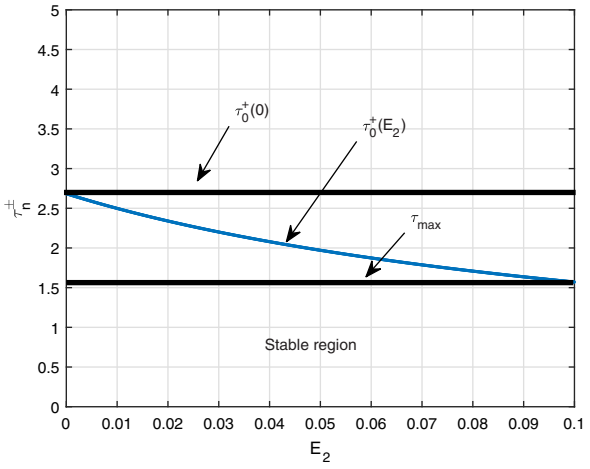


**Fig. 3.** The curve $\tau = \tau_0^+(E_2)$ separates the stability and instability region in the $E_2\tau$-plane. The change of stability due to different levels of harvesting are visible.

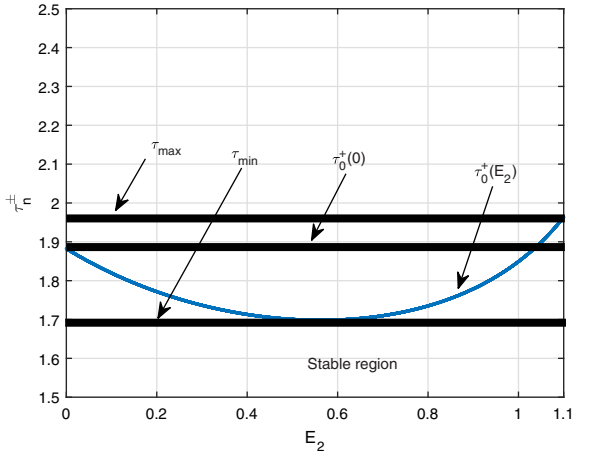


**Fig. 4.** The region below the blue curve $\tau = \tau_0^+(E_2)$ is the region of stability and above the curve is the instability region in the $E_2\tau$-plane. Because of the concave upward nature of $\tau = \tau_0^+(E_2)$, harvesting induced stability switching occurs. (For interpretation of the references to color in this figure legend, the reader is referred to the web version of this article.)

(i) For $\mathcal{T}$ lying between $(0, \tau_{\max})$, the coordinate $(E_2, \mathcal{T})$ stays in the region of stability for all effort, as can be seen from the Fig. 3. Hence, harvesting cannot destabilize the system.

(ii) For $\mathcal{T} \in (\tau_{\max}, \tau_0^+(0))$, the coordinate $(E_2, \mathcal{T})$ stays in the stability region for smaller effort, but with increasing effort, the coordinate enters into the region of instability as is clear from the Fig. 3. Hence, the unharvested system which was stable can be changed to instability, and the stability cannot be regained under increasing harvesting.

(iii) For $\mathcal{T} > \tau_0^+(0)$, the coordinate $(E_2, \mathcal{T})$ remains in the unstable region throughout. Thus, the instability will persist for any effort.

The above observation reveals that predator harvesting does not stabilize the system when the unharvested system is in the unstable mode. Unlike prey harvesting (Fig. 1 in Section 2.2.1), which have stabilized the unstable system, predator harvesting have a destabilizing effect.

We consider the parameters sets as is taken in Example 2.1 which satisfies the condition $\tau_0^+(0) < \tau_1^+(0) < \tau_0^-(0)$. The harvesting effort should lie in the range (0, 1.1) for co-existence of species. The solid blue curve represent $\tau = \tau_0^+(E_2)$ (see Fig. 4) which is unimodal with a minimum value $\tau_{\min}$. The

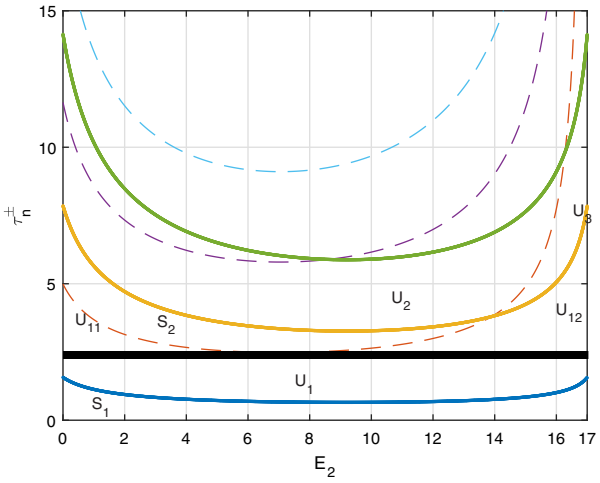


**Fig. 5.** Stability and instability regions are separated by the solid curves and dashed curves. Different stability and instability regions are identified to examine the stability changes.

region enclosed by the $E_2$-axis and $\tau = \tau_0^+(E_2)$ is the region of stability and the whole region afterwards is the region of instability. The curves $\tau = \tau_{\min}$, $\tau = \tau_{\max}$, $\tau = \tau_0^+(0)$ are plotted accordingly where $\tau_{\max} = \lim_{E_2 \to 1.1} \tau_0^+(E_2)$. The following stability behavior was observed based on the chosen $\mathcal{T}$ value.

(i) For $\mathcal{T}$ lying between $(0, \tau_{\min})$, the coordinate $(E_2, \mathcal{T})$ stays in the region of stability for all effort as can be seen from Fig. 4. Thus, harvesting has no influence over the stability of the system.
(ii) For $\mathcal{T} \in (\tau_{\min}, \tau_0^+(0))$, the coordinate $(E_2, \mathcal{T})$ is stable for smaller effort but with increasing harvesting pressure, enters the instability region and again shifts to the stability region for larger effort. Hence, harvesting induces stability switching in the system.
(iii) For $\mathcal{T} \in (\tau_0^+(0), \tau_{\max})$, the coordinate $(E_2, \mathcal{T})$ shifts from region of instability to region of stability when effort is significantly large. Henceforth, harvesting can remove the instability prevailing in the unharvested system.
(iv) For $\mathcal{T} > \tau_{\max}$, the coordinate $(E_2, \mathcal{T})$ remains in the unstable region throughout. Hence, harvesting cannot change the instability for any effort.

The above discussion infers that harvesting stabilizes the system beyond some critical effort unlike the previous case of predator harvesting (Fig. 3). Further, stability switching can be experienced in this case which was absent in the previous cases of prey and predator harvesting (Fig. 1 in Section 2.2.1 and Fig. 3).

***Case II: When the unharvested system experiences delay induced stability switching***

Now we are going to investigate the harvesting impact when the unharvested system exhibits delay induced switching. Taking all the values of $r$, $K$, $m$, $\alpha$, $\beta$ as in Example 2.2 for the unharvested system (1), it is observed that the system experiences eight stability switching due to delay. Introducing predator harvesting in the system (5), the effort of harvesting $E_2$ for existence of interior equilibrium was found to be lying in the range (0, 17). The solid curves and dashed curves represents $\tau = \tau_n^+(E_2)$ and $\tau = \tau_n^-(E_2)$, $(n = 0, 1, 2, \ldots)$, respectively corresponding to increasing effort (see Fig. 5). Also the solid horizontal black curve is the curve $\tau = \tau'_{\min}$, where $\tau'_{\min}$ is the minimum of $\tau_0^-(E_2)$. The region $S_1$ enclosed between the $E_2$-axis and the solid blue curve $\tau = \tau_0^+(E_2)$ is the region of stability. The region enclosed by any solid curve and succeeding dashed curve is the region of instability. The region bounded by any dashed curve and succeeding solid curve above is the region of stability until intersection takes place between these two curves for increasing effort. After the intersection there will be simultaneous appearance of two solid curves. These consecutive appearance of two solid curves results in instability regions between the curves as well as regions above the curves for that particular range of $E_2$. According to the closed regions enclosed by the horizontal black curve and $\tau_n^{\pm}(E_2)$, regions $U_1, U_{11}, U_{12}, S_2, U_2$ and $U_3$ are defined as follows.

(i) $U_1$ is the closed region of instability enclosed between the black horizontal curve and $\tau = \tau_0^+(E_2)$ curve.
(ii) $U_{11}$ is the closed region of instability enclosed between the horizontal black curve and $\tau = \tau_0^-(E_2)$ curve.
(iii) $U_{12}$ is also the closed region of instability enclosed between the horizontal black curve, $\tau = \tau_0^-(E_2)$ and $\tau = \tau_1^+(E_2)$ curve.
(iv) $S_2$ is the closed region of stability enclosed between $\tau = \tau_0^-(E_2)$ and $\tau = \tau_1^+(E_2)$.
(v) $U_2$ is the closed region of instability enclosed between $\tau = \tau_1^+(E_2)$, $\tau = \tau_1^-(E_2)$, $\tau = \tau_2^+(E_2)$, and $\tau = \tau_0^-(E_2)$.
(vi) $U_3$ is the closed region of instability enclosed between $\tau = \tau_1^+(E_2)$, $\tau = \tau_0^-(E_2)$.

Now it can be seen in the Fig. 5 that, for $\mathcal{T} \in (0, \tau_0^+(0))$, the stability behavior will be same as was explored in the previous case of predator harvesting (see Fig. 4).

Some of the other significant stability behaviors (including harvesting induced stability switching), that can be noticed, are as follows.

(i) For $\mathcal{T} \in (\tau^*, \tau'_{\min})$ (where $\tau^* = \max\{\tau_0^+(0), \tau_{\max}\}$ with $\tau_{\max} = \lim_{E_2 \to E^*} \tau_0^+(E_2)$ and $E^* = K\beta - m$), instability of the system will persist throughout and hence, harvesting cannot stabilize the system.
(ii) For $\mathcal{T} \in (\tau'_{\min}, \tau''_{\min})$, where $\tau''_{\min}$ is the minimum value of $\tau_1^+(E_2)$ (the solid yellow curve), the system experiences instability switching because of the shifting of the coordinate $(E_2, \mathcal{T})$ from region $U_{11}$ to $S_2$ to $U_{12}$.

*2.2.3. Maximum sustainable yield and stability*

In this subsection, we study the influence of MSY policy in the Lotka–Volterra type model under predator harvesting. As prey harvesting towards MSY drive the predator populations to extinction, we focus our analysis for predator harvesting at MSY level. It is well established fact, that the co-existing equilibrium is globally stable in non-delayed LV type predator-prey model and hence, harvesting the predators at MSY level maintain the stability as well [29]. We would like to know whether such stability result is generic when the unharvested system involves time delay factor.

The interior steady state for predator harvesting is given as:

$$(x^*, y^*) = \left( \frac{m + E_2}{\beta}, r\left( \frac{K\beta - m}{K\alpha\beta} - \frac{E_2}{K\alpha\beta} \right) \right).$$

For co-existence of the interior steady state, the effort $E_2$ must lie in the range $(0, K\beta - m)$. The yield at the equilibrium is:

$$\begin{aligned} Y(E_2) &= E_2 y^* \\ &= E_2 r\left( \frac{K\beta - m}{K\alpha\beta} - \frac{E_2}{K\alpha\beta} \right). \end{aligned}$$

As $Y(E_2)$ is a quadratic function in $E_2$, it must attend a maximum when

$$E_2^{MSY} = \frac{K\beta - m}{2}.$$

From the above expression, it is clear that MSY is achieved at equilibrium and $E_2^{MSY}$ lies at the middle of the effort range for

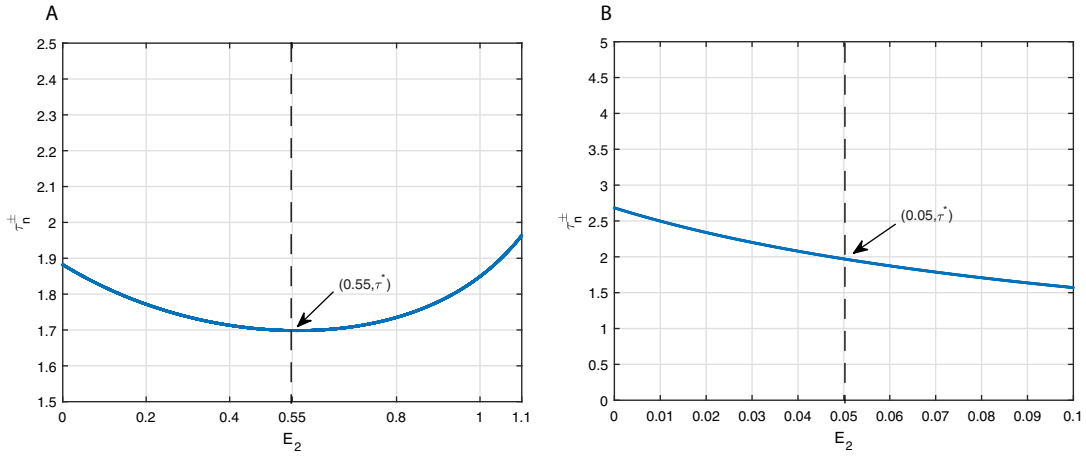


**Fig. 6.** The blue curves represent $\tau = \tau_0^+(E_2)$ and the vertical curves represent $E_2 \equiv E_2^{MSY} = \frac{K\beta - m}{2}$. The lower region of $\tau = \tau_0^+(E_2)$ is the region of stability. (a) and (b) are depicted for two different parameter sets. It is shown that the system may lose its stability when harvest quota is set at MSY level. (For interpretation of the references to color in this figure legend, the reader is referred to the web version of this article.)

which both populations persist. However, our interest is to establish whether the system is stable at MSY harvest limit. In this context, we recall Figs. 3 and 4. Now we plot the vertical doted curve $E_2 = (K\beta - m)/2$ in the $E_2 - \tau^{\pm}$ plane along with the curve $\tau = \tau_0^+(E_2)$ in both the figures and rename them as Fig. 6(a) and (b), respectively.

We assume that the curve $E_2 = \frac{K\beta - m}{2}$ and $\tau = \tau_0^+(E_2)$ intersect at $(E_2^{MSY}, \tau^*)$ in both the figures. The following stability phenomenon can occur.

a. If $\mathcal{T} < \tau^*$ in the unharvested system, then the coexisting equilibrium is stable. In that case, harvesting at MSY produces a stable stock.
b. If $\mathcal{T} \in (\tau^*, \tau_0^+(0))$ in the unharvested system, then the coexisting equilibrium is stable as well. In that case, harvesting at MSY does not produce a stable stock.
c. If $\mathcal{T} > \tau_0^+(0)$ in the unharvested system, the coexisting steady state is unstable and the equilibrium stock towards MSY harvest level remains unstable.

Thus, there is no guarantee that the system maintain stability towards the maximum yield, if the unharvested system is stable. On the other hand, MSY does not exist at stable state when the unharvested system is unstable. Similar phenomenon occurs even when we consider more complex parametric situation corresponding to the Fig. 5. However, in more complex case, we observe that harvesting the predator at MSY promotes stability even when the unharvested system is unstable. This result can be explained by considering the regions $U_{11}$ and $S_2$ in Fig. 5. Under the considered explanation, $E_2^{MSY} = 8.5$. One can choose $\mathcal{T} = 3$ in the unharvested system. Then the system becomes unstable (link with the left side vertical boundary of the unstable region $U_{11}$). However, if we employ effort at $E_2^{MSY}$, the system becomes stable (corresponds to the stability region $S_2$).

## 3. Rosenzweig–MacArthur model

It is always difficult task to investigate complicated mathematical models analytically. To avoid such complexities, theoretical ecologists always prefer to propose simple Lotka–Volterra or Lotka-Volterra type [28,29] predator-prey systems and validate the results in more general ecological systems. In this section, we explore results in the Rosenzweig–MacArthur predator-prey system. The aim of this analysis is to understand the generality of the outcomes obtained from our earlier Lotka–Volterra type system.

In fact, unlike LV type model, RM model can exhibit oscillations [43]. Very recently, several harvesting results in RM model without time delay are discussed by Ghosh et al. [10] and Tromeur and Loeuille [51]. On the other hand, delayed RM model [20] and in general Gause-type predator-prey system [35] are investigated in order to explain harvesting impact. In the succeeding section, we discuss the delay induced dynamics in the RM model.

### 3.1. Dynamics of delayed RM model

In this section, we consider a delayed RM model:

$$\dot{x} = rx\left(1 - \frac{x(t-\tau)}{K}\right) - \frac{\alpha xy}{h+x},$$

$$\dot{y} = \frac{\beta xy}{h+x} - my, \tag{17}$$

where $x(t), y(t), r, K, \alpha, \beta, m$ denotes the same notation as mentioned in the previous sections and $h$ stands for half capturing saturation constant.

The interior equilibrium of the model is

$$(x^*, y^*) = \left(\frac{mh}{\beta - m}, \frac{h\beta}{\alpha(\beta - m)}\left(r - \frac{rmh}{K(\beta - m)}\right)\right),$$

provided $\beta > m$ and $K(\beta - m) > mh$.

Linearizing the system near interior equilibrium, we obtain the characteristic equation,

$$\lambda^2 + a_1\lambda + a_2\lambda e^{-\lambda\tau} + a_3 = 0, \tag{18}$$

where

$$a_1 = -\frac{\alpha x^* y^*}{(h+x^*)^2},$$

$$a_2 = \frac{rx^*}{K},$$

$$a_3 = \frac{h\alpha\beta x^* y^*}{(h+x^*)^3}.$$

We are using the same notation for coefficient in the characteristic equation as mentioned in [20]. Clearly $a_2$ and $a_3$ are positive and $a_1$ is negative. The characteristic equation for $\tau = 0$ becomes

$$\lambda^2 + (a_1 + a_2)\lambda + a_3 = 0,$$

i.e.

$$\lambda = \frac{-(a_1 + a_2) \pm \sqrt{(a_1 + a_2)^2 - 4a_3}}{2}.$$

The equilibrium of the non-delayed system is asymptotically stable if $a_1 + a_2 > 0$.

Martin and Ruan [35] and Kar [20] stated that three possible cases concerning the stability changes due to delay are as follows.

**Result 1** The equilibrium of the system will be asymptotically stable for all time delay if $a_1 + a_2 > 0$ and $a_1^2 - a_2^2 - 2a_3 > 0$.

**Result 2** The equilibrium will be asymptotically stable only up to some time delay, beyond which it will be unstable if $a_1 + a_2 > 0$, $a_2^2 - a_1^2 + 2a_3 > 0$ and $(a_2^2 - a_1^2 + 2a_3)^2 = 4a_3^2$.

**Result 3** The equilibrium will experience delay induced switching of stabilities if $a_1 + a_2 > 0$, $a_2^2 - a_1^2 + 2a_3 > 0$ and $(a_2^2 - a_1^2 + 2a_3)^2 > 4a_3^2$.

In fact, the parameter conditions in the above statement are due to Kar [20], but Martin and Ruan [35] have proposed the same conditions with different notations. Martin and Ruan [35] believed that such a parameter condition is possible in model, where delay never causes instability. The first result proposed by Kar [20] in RM model is not observed in our LV type model. Therefore, we would like to revisit if delay really has an influence to maintain stability in the RM model.

To check for the change of dynamics due to time delay, we assume that there exists $\lambda = i\omega$ $(\omega > 0)$ for some critical $\tau$. Then the characteristics Eq. (18), after separating the real and imaginary parts, can be written as,

$$-\omega^2 + \omega a_2 \sin(\omega\tau) + a_3 = 0 \tag{19a}$$

$$a_1\omega + a_2\omega\cos(\omega\tau) = 0. \tag{19b}$$

Let us define,

$$\theta_1 = \arccos\left(-\frac{a_1}{a_2}\right), 0 < \theta_1 < \frac{\pi}{2},$$

$$\theta_2 = \arccos\left(-\frac{a_1}{a_2}\right), \frac{3\pi}{2} < \theta_2 < 2\pi.$$

Like in the previous section, accordingly for the choice of $\theta_1$ and $\theta_2$, we get two different values of $\sin(\omega\tau)$, and the corresponding values of $\omega$ can be given from (19b) as,

$$\omega_+ = \frac{1}{2}\sqrt{a_2^2 - a_1^2} + \frac{1}{2}\sqrt{a_2^2 - a_1^2 + 4a_3}, \tag{20}$$

$$\omega_- = -\frac{1}{2}\sqrt{a_2^2 - a_1^2} + \frac{1}{2}\sqrt{a_2^2 - a_1^2 + 4a_3}. \tag{21}$$

Since $a_1 < 0$, $a_2 > 0$, $a_1 + a_2 > 0$ (i.e., $|a_2| > |a_1|$), both $\omega_+$ and $\omega_-$ are positive.

The corresponding $\tau$ will be given as,

$$\tau_n^+ = \frac{\theta_1 + 2n\pi}{\omega_+},$$

$$\tau_n^- = \frac{\theta_2 + 2n\pi}{\omega_-}.$$

Thus, there exist such $\omega$'s for which Hopf-bifurcation occurs and hence, increasing time delay cannot maintain stability. This addresses the second major issue we have posed in the Introduction section.

Our analysis claims that, the first result does not hold, as mentioned in the existing literature, but the second result can be observed in LV type as well as RM model.

However, we show that the parameter conditions due to Kar [20] and Martin and Ruan [35] in the second result are sufficient, but not necessary. It can be seen from the example given below:

**Example 3.1.** Let us consider the parameter sets as $r = 0.8$, $K = 45$, $\alpha = 0.7$, $\beta = 0.4$, $h = 10$, $m = 0.3$. Then, the given parameter sets satisfies the conditions $(a_2^2 - a_1^2 + 2a_3)^2 > 4a_3^2$ including remaining ones corresponding to the Result 2. But, the equilibrium (30, 15.23) exhibits stable dynamics when $\tau < 2.23$ and at $\tau = 2.23$ (approx) Hopf-bifurcation occurs. The system will be unstable for $\tau > 2.23$. In fact, transversality condition is satisfied at the critical time delay.

It shows that the condition mentioned in Result 2 is sufficient, but not necessary. Importantly, as the above parameters now satisfied the conditions related to the Result 3 and we could have obtained stability switching based on the proposed theory due to Kar [20], Kar and Pahari [24] and Martin and Ruan [35], but we simply observed a stability change for increasing time delay. Hence, condition for stability switching in [20,24] and [35] (also see [24]) is not true always.

The condition for the existence of stability switching in LV type models is discussed in Theorem 2.2. Therefore, Theorem 2.2 suggests that an additional parametric condition is required for stability switching which can be obtained from the inequalities. To understand the stability switching phenomenon in RM model we present the following example.

**Example 3.2.** We set $r = 0.25$, $K = 10$, $\alpha = 1.5$, $\beta = 1.3$, $h = 10$ and $m = 0.1$. The ecological parameters are chosen in such a way that it satisfies the parametric restrictions given in Result 3 including $\tau_1^+ > \tau_0^-$ (additional condition). The condition, $\tau_1^+ > \tau_0^-$ ensures the existence of at least one stability switch. The values of $\tau$ for which bifurcation occurs, are shown as follows. We obtained 2 stability switching in the unharvested model.

$$\begin{array}{ll} \tau_0^+ \approx 3.7198 & \tau_0^- \approx 40.8656 \\ \tau_1^+ \approx 45.3025 & \tau_1^- \approx 85.7461 \\ \tau_2^+ \approx 86.8852 & \tau_2^- \approx 130.6266 \\ \tau_3^+ \approx 128.46790 & \end{array}$$

Therefore, we have improved the delay induced stability results and established new parameter condition for the stability switching compared to the earlier articles. The major observation is that both the LV and RM models exhibit similar stability behavior due to time delay.

### 3.2. Harvesting results in RM model

Now we would like to know if the delayed RM model also produces similar outcomes such a LV type model under harvesting. In the following subsections, we will study the effect of harvesting in the dynamics of the RM system by considering a fixed time delay. In addition, we establish whether maximum harvest from predator populations can stabilize the system.

Our main interest is to explore harvesting results when the unharvested system is at non-equilibrium state. Although the non-delayed RM model can exhibit cyclic dynamics due to Holling type II functional response and such a system is extensively studied by Ghosh et al. [10]. However, if the system is in oscillatory mode due to functional response, time delay does not have any role to change stability (Follows from Section 3.1). Here, we assume that the unharvested system becomes unstable due to time delay only and hence, we need to restrict the ecological parameters accordingly for which non-delay RM model leads a stable equilibrium.

Before starting the analysis for harvesting, the natural system must meet the parametric conditions provided in the Results 2 or 3 as described in Section 3.1. The dynamics of the unharvested system corresponding to the second result is simple and we have verified that it leads to the similar results obtained from LV type model. Thus, we focus our study when the unharvested system experiences more complex dynamics such as delay induced stability switching based on the Result 3.

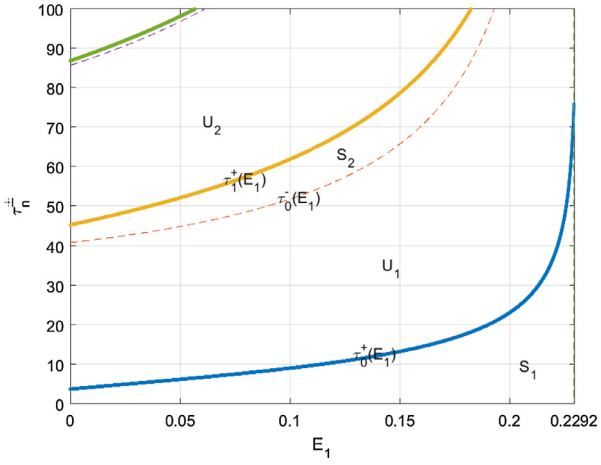


**Fig. 7.** The curves $\tau = \tau_n^{\pm}(E_1)$ increase in $E_1$. Because of increasing nature of $\tau = \tau_0^{+}(E_1)$, harvesting has a stabilizing effect when the unharvested system involves smaller time delay. The results will be significantly different if the time delay is comparatively larger.

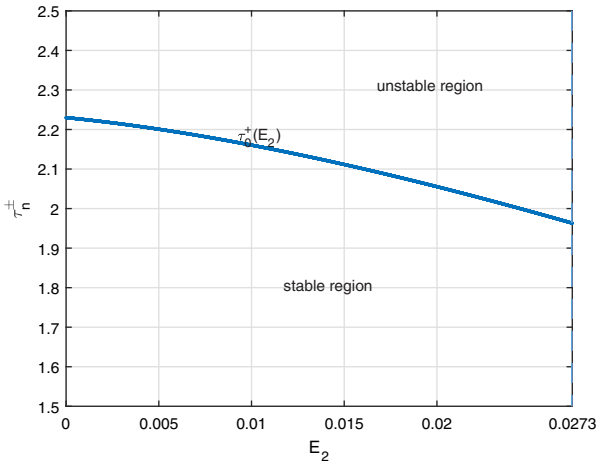


**Fig. 8.** The curve $\tau = \tau_0^{+}(E_2)$ decreases in $E_2$. If the unharvested system is unstable due to fixed time delay, harvesting does not have any effect to stabilize it. If the unharvested system is stable for intermediate time delay, harvesting can destroy the stability.

*3.2.1. Prey harvesting*

The Rosenzweig–MacArthur model with constant time delay $\mathcal{T}$ in the prey specific growth rate subjected to prey harvesting is given as:

$$\dot{x} = rx\left(1-\frac{x(t-\tau)}{K}\right)-\frac{\alpha xy}{h+x}-E_1x,$$
$$\dot{y} = \frac{\beta xy}{h+x}-my. \tag{22}$$

The interior equilibrium for the system (22) and the corresponding approach to determine the time delays for which Hopf-bifurcation occurs is similar as in the previous section. Hence, the details are given in Appendix A.

To perform numerical simulations, we use the parameters given in Example 3.2. We have already explained that these parameters show 2 stability switching in the unharvested system. The coexisting equilibrium is computed as (0.833, 1.655), which is asymptotically stable. The range of employed effort should be (0, 0.2292), in order to maintain the persistence of both the populations.

Likewise previous section, the solid curves and dashed curves, in Fig. 7, represents $\tau = \tau_n^{+}(E_1)$ and $\tau = \tau_n^{-}(E_1)$, $(n = 0,1,2,\ldots)$, respectively, corresponding to increasing effort. The closed regions $S_n$, $(n = 1, 2)$, are the regions of stability and $U_n$, $(n = 1, 2, 3)$ are the regions of instability. Clearly, $\tau$-axis (i.e. $E_1 = 0$) in Fig. 7 shows that stability switching occurs in the unharvested model.

Similar stability behaviors as that in Lotka–Volterra model was observed, which are discussed below.

(i) For $\mathcal{T} \in (0, \tau_0^{+}(0))$, the coordinate $(E_1, \mathcal{T})$ remains in the stability region $S_1$ (region enclosed between the $E_1$-axis and the curve $\tau = \tau_0^{+}(E_1)$) throughout for all effort.

(ii) For $\mathcal{T} \in (\tau_0^{+}(0), \tau_0^{-}(0))$, the coordinate $(E_1, \mathcal{T})$ stays in the instability region $U_1$ (region enclosed between the curves $\tau = \tau_0^{+}(E_1)$ and $\tau = \tau_0^{-}(E_1)$) initially for some small effort after which it shifts to the stability region $S_1$ i.e. the system can be stabilized by some effort and thus harvesting have a stabilizing effect on the system.

(iii) For $\mathcal{T} \in (\tau_0^{-}(0), \tau_1^{+}(0))$, the system experiences stability switching with increasing effort as can be seen by the shifting of the coordinate $(E_1, \mathcal{T})$ from regions $S_2$ (region enclosed between the curve $\tau = \tau_0^{-}(E_1)$ and $\tau = \tau_1^{+}(E_1)$) to $U_1$ and then from $U_1$ to $S_1$ in Fig. 7.

(iv) For $\mathcal{T} \in (\tau_{\max}, \tau_1^{-}(0))$, the coordinate $(E_1, \mathcal{T})$ experiences instability switching with effort, as can be seen from the shifting of the coordinate $(E_1, \mathcal{T})$ from the instability regions $U_2$ (region enclosed between $\tau = \tau_1^{+}(E_1)$ and $\tau = \tau_1^{-}(E_1)$) to stability region $S_2$ and again from $S_2$ to instability region $U_1$, where $\tau_{\max} = \lim_{E_1 \to E^*} \tau_0^{+}(E_1))$, $E^* = \frac{r}{q}(1 - \frac{mh}{K(\beta - m)})$ and $\tau_1^{-}(E_1)$ is the dashed curve succeeding $\tau_1^{+}(E_1)$.

*3.2.2. Predator harvesting*

The Rosenzweig–MacArthur model with constant time delay $\mathcal{T}$ in the prey specific growth rate under predator harvesting is given as:

$$\dot{x} = rx\left(1-\frac{x(t-\tau)}{K}\right)-\frac{\alpha xy}{h+x},$$
$$\dot{y} = \frac{\beta xy}{h+x}-my-E_2y. \tag{23}$$

The interior equilibrium for the system (23) and the corresponding process to find the time delays for which Hopf-bifurcation occur is similar as in the previous section and is given in Appendix B.

We rely on numerical simulations to observe the different dynamical natures that occurs due to different range of time delays incorporated in the model under prey harvesting.

We will be considering two cases. First will be the case without switching and second will be the case of switching.

***Case I: When the unharvested system does not experience delay induced stability switching***

Taking the same parameter set as in Example 3.1, we determine the range of the effort under predator harvesting as (0, 0.0273). The unharvested system does not experience any switching of stability, as can be seen from Example 3.1. For $\tau < 2.23$, the unharvested system is stable but for $\tau > 2.23$, it is unstable and Hopf-bifurcation occurs at $\tau = 2.23$. In Fig. 8, we have drawn $\tau_0^{+}(E_2)$ which creates the region of stability and instability. The curve is decreasing in effort. It leads that the unharvested stable system can be destabilize under harvesting. On the other hand, the system remains unstable under harvesting if the unharvested system is unstable. Although, Kar and Pahari [24] concluded it by taking two distinct efforts numerically, we have now shown a complete picture for whole range of effort. Now we focus in the

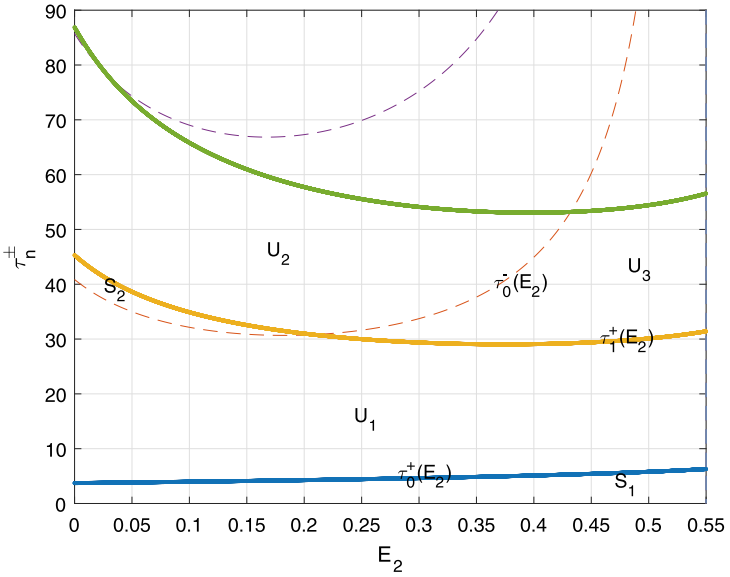


**Fig. 9.** Different regions are depicted to describe the stability nature by plotting the curves $\tau = \tau_n^{\pm}(E_2)$. The curve $\tau = \tau_0^{+}(E_2)$ is increasing in nature and hence, a stable pre-harvested system incorporating smaller time delay maintains its stability under any level of harvesting effort.

second case where some different results will hold for predator harvesting.

***Case II: When the unharvested system experiences delay induced stability switching***

We obtain the effort range for predator harvesting as (0, 0.55), when we set the ecological parameters given in Example 3.2. In the Fig. 9, the solid curves and dashed curves represents $\tau = \tau_n^{+}(E_2)$ and $\tau = \tau_n^{-}(E_2)$, $(n = 0,1,2,\ldots)$ respectively, corresponding to increasing harvesting effort. The considered parameters established the stability switching phenomenon in the unharvested case which can be seen from $\tau$-axis (i.e. $E_2 = 0$). The region enclosed between the $E_2$-axis and the first solid curve is the region of stability. The region enclosed by any solid curve and succeeding dashed curve is the region of instability. The region bounded by any dashed curve and succeeding solid curve above is the region of stability until intersection takes place between these two curves for increasing effort. After the intersection there will be simultaneous appearance of two solid curves. These consecutive appearance of two solid curves results in instability regions between the curves as well as regions above the curves for that particular range of $E_2$.

Few of the stability behaviors that can be observed based on the chosen value of $\mathcal{T}$ for the system (23) is given as follows.

(i) For $\mathcal{T} = 1$, the coordinate $(E_2, \mathcal{T})$ remains in the stable region $S_1$ throughout. Thus harvesting have no destabilizing effect on the system.
(ii) For $\mathcal{T} \in (10, 20)$, the unharvested system will be unstable and no amount of harvesting can stabilize the system (analysis follows from the unstable region $U_1$).
(iii) For $\mathcal{T} = 42$, the coordinate $(E_2, \mathcal{T})$ shifts from region of stability $S_2$ to regions $U_2$ and $U_3$, both of which are region of instability. Hence harvesting have a destabilizing effect on the system.
(iv) For $\mathcal{T} = 35$, unharvested system is unstable. But increasing effort of harvesting can induce instability switching.

### 3.2.3. Maximum sustainable yield and stability

When predator populations are exploited, the effort does not exceed $(\beta K/(K+h) - m)$ for coexistence of populations. The yield

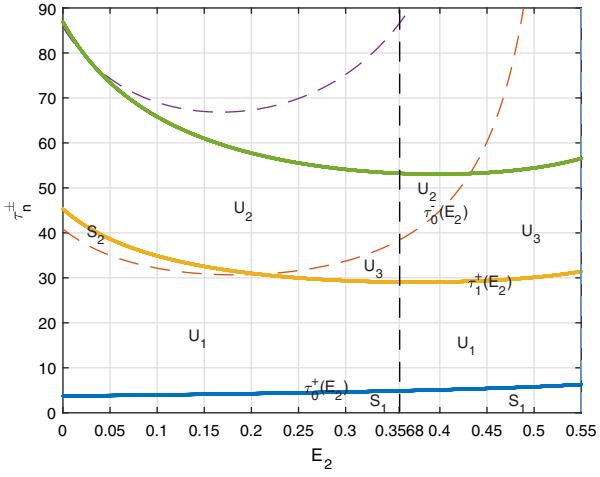


**Fig. 10.** The dashed vertical curve $E = E_2^{MSY}$ passes through regions of stability and instability. The curve mostly passes through the instability region. The stock corresponding to MSY is stable only when the time delay is smaller.

at equilibrium is given as:

$$Y(E_2) = E_2 y^* = \frac{E_2 h\beta}{\alpha(\beta - m - E_2)}\left(r - \frac{rh(m+E_2)}{K(\beta - m - E_2)}\right).$$

The maximum yield is obtained at equilibrium when

$$E_2 = E_2^{MSY} = \frac{(\beta - m)(K(\beta - m) - hm)}{(K(\beta - m) - hm + 2h\beta)}.$$

Corresponding to the Fig. 9, the range of effort for which both species coexist is (0, 0.55). In this case, $E_2^{MSY} = 0.3568$. Unlike the case of LV type model, $E_2^{MSY}$ in RM model does not lie at the middle of the effort range. We now recall the Fig. 9 and draw $E_2 = E_2^{MSY}$ (see Fig. 10). It is a vertical line and crosses many stability and instability regions. It is clear that, when time delay is very small (for instance, $\mathcal{T} = 1$) in the unharvested system, the equilibrium is stable. Therefore, Fig. 10 reveals that harvesting the predator towards MSY maintains stability (corresponds to the region $S_1$). Similarly, if the time delay $\mathcal{T} = 43$, the equilibrium of the

unharvested system is asymptotically stable. But harvesting at MSY level does not stabilize the system. If the time delay in the unharvested system is slightly greater than $\tau_0^+$, then the system is unstable. In this case, harvesting the predator towards MSY induces stability in the system (because, the curve $\tau = \tau_0^+(E_2)$ increases). Otherwise, simulations demonstrates that the system towards MSY cannot be stabilized if the unharvested system is unstable due to time delay.

## 4. Discussion and conclusion

In this paper, we have analyzed both the LV type and RM predator-prey models incorporating time delay in the logistic growth function. First, we have explained the dynamics of the unharvested systems due to delay. As the time delay does not change in fast time scale compared to the change in harvesting effort, we fix time delay as constant when effort is exerted. Delay induced stability is investigated in both the models by many researchers [17,20,24,35,48,49], but we have observed some new results. Martin and Ruan [35] presented three different stability results due to time delay in a generalized Gause-type predator-prey model (see Section 3.1 in this article). However, only the occurrence of stability switching phenomenon is investigated by Ho and Ou [17], Toaha and Hassan [48] and Toaha et al. [49]. We have proved that time delay can induce instability, for some critical value, and the instability persists if the delay exceeds the critical threshold. Hence, stability switching is not the only phenomenon in LV type and RM models. In addition, we observed that time delay certainly causes instability in LV type system. However, Martin and Ruan [35] and Kar and Pahari [24] proved that there exists parametric condition, for which, time delay does not change the asymptotic stability behavior of the coexisting equilibrium. Here, we have shown that such a parameter condition is not possible in RM model, for which steady state remain stable for increasing time delay. Likewise, the LV model, RM model also experiences instability for some critical value and the coexisting equilibrium stays unstable for larger time delay. Therefore, we can now suggest that both the models have qualitatively similar dynamics under time delay.

It is customary that ecologists always propose simple models and drive more general results which can be consistent with more complex models. For example, Legović et al. [29] studied only LV type predator-prey system and established the extinction of population at MSY level in more complex and multi-species food chain. Recently, Pilyugin [42] examined the variation of population biomass due to protected area by considering a LV model to address the impact of marine reserve in more general sense. Although, LV and LV type models are sometimes criticized because of its simplicity, but they can drive many ecological theories. Hence, it was important for us to prove that the delay induced dynamics are similar for both LV type and RM models, so as to verify whether generalized harvesting results can be obtained for both the models. However, we conclude from the following discussion that many of the harvesting results are similar in both the LV type and RM models.

It is generally accepted that, harvesting stabilize a system when the unharvested system is at non-equilibrium state [27] due to nonlinear functional response. Numerical simulations reveals that harvesting the prey or predator can destroy oscillation in a system under additional food [22]. In fact, Ghosh et al. [10] and Tromeur and Loeuille [51] established the fact that prey and predator harvesting can stabilize a non-equilibrium dynamics in non-delayed Rosenzweig–MacArthur predator-prey system. If the equilibrium of the unharvested system stay stable, then harvesting does not have any influence to destabilize it. On the other hand, Martin and Ruan [35] showed that harvesting the prey population can stabilize a system if the unharvested system is in non equilibrium state due to time delay. Kar and Ghorai [21] and Meng et al. [38] have observed that prey harvesting stabilized a system when the unharvested system is at unstable state. In our LV type model, we found that prey harvesting can have several impacts depending upon delay induced dynamic mode of the unharvested system.

(i) Harvesting does not have any influence to destabilize when the unharvested system is stable due to smaller time delay (See Fig. 1).
(ii) If an unharvested is at unstable mode due to moderate size of time delay, larger harvesting effort can stabilize the system (See Fig. 1).
(iii) If the time delay is larger and unharvested system is unstable, then it may not be stabilized by harvesting (See Fig. 1).
(iv) If the unharvested system for a fixed time delay is stable, harvesting can induce stability switching (See Fig. 2).
(v) If the unharvested system for a fixed time delay is unstable, harvesting can induce instability switching (See Fig. 2).

Some of the above results are proved to be consistent for delayed RM model under complex parameter setting, and the rest are verified (not shown in the paper) in simple parameter condition. It is probably believed that, prey harvesting causes stability if unharvested system is unstable due to functional response [10,13,51] or due to time delay [21,35,38]. Of course, Meng et al. [38] have studied Beddington-DeAngelis model with delay dependent coefficient, whereas our models are different from [38]. However, our results show that many other phenomenon may be exhibited based on the dynamics of unharvested system and particular model selection. In this context, our investigation is attractive.

In the context of predator harvesting, we would like to mention Kar and Ghorai [21] and Meng et al.'s [38] contribution. These are the only two research groups who have observed that predator harvesting stabilize a system when the unharvested system is at unstable mode. In our LV type model, we found the following results:

(i) Harvesting does not have any influence to destabilize when the unharvested system is stable system due to smaller time delay (See Figs. 3 and 4). Such a result is also true for prey harvesting.
(ii) If an unharvested is at stable mode due to moderate size of time delay, larger harvesting effort induce instability (See Fig. 3). This does not happen in the case of prey harvesting.
(iii) If a system is at stable mode prior to harvesting, harvesting the predator can induce stability switching (see Fig. 4).
(iv) If the time delay is large enough and unharvested system is unstable, then it may not be stabilize by harvesting (See Figs. 3–5).
(v) Likewise the prey harvesting, predator harvesting can produce stability switching (See Fig. 5).
(vi) If the unharvested system for a fixed time delay is unstable, the harvested system can experiences instability switching for increasing effort (See Fig. 5). We would like to remind that instability switching is identified in a non-delayed tritrophic food chain when top-predator is exploited [13].

It is observed that prey and predator harvesting do not produce same results. Some of the above results for predator harvesting in LV type model are same with the RM model. However, we could not identify the stability and instability switching phenomenon when predator is exploited in RM model (see Fig. 9). Our investigation leads to new outcomes compared to the existing observations by Meng et al. [38] and Kar and Ghorai [21].

Readers might think that harvesting results can be derived by just varying the time delay with a fixed effort. As we mentioned that harvested systems are analyzed by some researchers using

this approach (for instance, [39]), one might think that harvesting induced stability switching happens because of delay induced stability switching. Thus, there is no need to examine the explicit impact of harvesting. Only delay induced dynamics is sufficient to know the harvesting effects. However, such concept may go wrong. In the RM model, we observed that the unharvested system experiences stability switching due to delay, but harvesting does not show any stability switching (see Fig. 9). Therefore, it was essential to know the explicit harvesting results as we have performed.

One might think about the impact of harvesting on both the species using combined effort. In fact, such approach is more realistic in fishery as a non-target species might be caught along with the target species. Although we have not paid attention by harvesting both the species, but we can infer the scenario from the individual prey and predator harvesting results. If the target species under combined effort is the prey (resp. predator), then the results will more likely to be coherent with the prey (resp. predator) harvesting case. We acknowledge Toaha et al. [49] for discussing a result based on combined effort. They mentioned that LV type harvested system becomes stable for a range of effort, then it becomes unstable and finally it regains stability for increasing effort (See Example 3.1 in their paper). Hence as per their description an stability switching occurs. Unfortunately, the unharvested system was unstable for $\tau = 1.8$. We have verified that an instability switching occurs in this case.

In a fishery, harvesting limit should reach at most MSY level for sustainability. The estimation for this MSY is quite easy in theoretical model when the harvested system is a steady state [8,9,29]. However, when the harvested system is at non-equilibrium state, it is quite challenging to measure the MSY [13]. In this case, stock or yield can be computed by time-averaged concept [36]. Perhaps, [10] is the first to prove that a non-delayed RM predator-prey system produces a stable stock at MSY (predator harvesting) regardless the dynamics of the unharvested system. In this view point and considering the research question proposed by Martin and Ruan [35], we examined the system dynamics when predator is exploited towards maximum yield. Based on LV type and RM model incorporating time delay reveals that:

(i) The system must produces stable stock at MSY level if the unharvested system is stable incorporating smaller time delay.
(ii) The system may not yield stable stock towards MSY if the unharvested system is stable with comparatively larger time delay.
(iii) The system is more likely to induce unstable stock to achieve MSY if the unharvested system is unstable due to time delay.

Hence, we are able to address the proposed work due to Martin and Ruan [35]. In the same time, we can claim that the rule established by Ghosh et al. [10] is not generic if the populations dynamics models may have very different types of non-equilibrium states.

The strength of these works are that (i) we have studied the harvesting impact in more systematic way and discussed all the possible phenomenon and (ii) we have explicitly derived many analytical condition on effort. However, we cannot claim that the above results always hold for any general predator-prey system including longer food chain. Outcomes might be slightly different for different models considered, but some of our results might be still valid. On the other hand, it might not be applicable directly to explain a specific case study as every case study must need very specific model as well. However, our discussion must contribute to enhance knowledge in explaining general results in theoretical and applied ecology. It would be interesting to study some widely different models with the same research theme for verifying our established results. In particular, we can examine whether stability switching phenomenon is possible due to harvesting in the model studied by Meng et al. [38] where one of the model coefficients depends on time delay.

## Declaration of interests

The authors declare that they have no known competing financial interests or personal relationships that could have appeared to influence the work reported in this paper.

## Acknowledgments

B.B. acknowledges the financial support from MHRD, Govt. of India, for her PhD programme. We appreciate the substantial comments and suggestions received from the eminent reviewers, which certainly helped to improve the content of the manuscript.

## Appendix A. Stability analysis for prey harvesting in RM model

The interior equilibrium of the model (22) is

$$(x^*, y^*) = \left(\frac{mh}{\beta - m}, \frac{h\beta}{\alpha(\beta - m)}\left(r - \frac{rmh}{K(\beta - m)} - E_1\right)\right).$$

The effort of harvesting for the existence of positive equilibrium must satisfy

$$0 < E_1 < r\left(1 - \frac{mh}{K(\beta - m)}\right). \tag{24}$$

Linearizing the system near interior equilibrium, we get the characteristics equation,

$$\lambda^2 + a_1\lambda + a_2\lambda e^{-\lambda\tau} + a_3 = 0, \tag{25}$$

where

$$a_1 = -\frac{\alpha x^* y^*}{(h+x^*)^2} = -\frac{m}{\beta}\left(r - \frac{rmh}{K(\beta - m)} - E_1\right),$$

$$a_2 = \frac{rx^*}{K} = \frac{rmh}{K(\beta - m)},$$

$$a_3 = \frac{h\alpha\beta x^* y^*}{(h+x^*)^3} = \frac{m}{\beta}(\beta - m)\left(r - \frac{rmh}{K(\beta - m)} - E_1\right).$$

Instead of distinct notations, we use the same notations used in Section 3.1. However, we have to remember that notations/ expressions depends on effort.

We have already checked for the stability of the system in non-delayed ($\tau = 0$) and non-harvested case in Section 3.1.

Now for $\tau \neq 0$, let us suppose there exist $\lambda = i\omega$ ($\omega > 0$). The characteristics Eq. (25) can be written as, (separating the real and imaginary parts)

$$-\omega^2 + \omega a_2 \sin(\omega\tau) + a_3 = 0, \tag{26a}$$

$$a_1\omega + a_2\omega\cos(\omega\tau) = 0. \tag{26b}$$

Let us define,

$$\theta_1 = \arccos\left(-\frac{a_1}{a_2}\right), 0 < \theta_1 < \frac{\pi}{2},$$

$$\theta_2 = \arccos\left(-\frac{a_1}{a_2}\right), \frac{3\pi}{2} < \theta_2 < 2\pi.$$

Accordingly, for the choice of $\theta_1$ and $\theta_2$, we get two positive values of $\omega$ given as,

$$\omega_+(E_1) = \frac{1}{2}\sqrt{a_2^2 - a_1^2} + \frac{1}{2}\sqrt{a_2^2 - a_1^2 + 4a_3}, \tag{27}$$

$$\omega_-(E_1) = -\frac{1}{2}\sqrt{a_2^2 - a_1^2} + \frac{1}{2}\sqrt{a_2^2 - a_1^2 + 4a_3}. \tag{28}$$

provided $a_2^2 - a_1^2 + 2a_3 > 0$ and $(a_2^2 - a_1^2 + 2a_3) > 4a_3^2$. The corresponding $\tau$ will be given as,

$$\tau_n^+(E_1) = \frac{\theta_1 + 2n\pi}{\omega_+},$$

$$\tau_n^-(E_1) = \frac{\theta_2 + 2n\pi}{\omega_-}.$$

We get different set of values of $\tau_n^{\pm}(E_1)$ based on the different effort of harvesting $E_1$.

## Appendix B. Stability analysis for predator harvesting in RM model

The interior equilibrium of the model (23) is

$$(x^*, y^*) = \left(\frac{h(m+E_2)}{\beta - m - E_2}, \frac{h\beta}{\alpha(\beta - m - E_2)}\left(r - \frac{rh(m+E_2)}{K(\beta - m - E_2)}\right)\right).$$

The effort of harvesting for the existence of positive equilibrium should be in the range

$$0 < E_2 < \beta\left(\frac{K}{K+h}\right) - m. \tag{29}$$

Linearizing the system near interior equilibrium, we get the characteristics equation,

$$\lambda^2 + a_1\lambda + a_2\lambda e^{-\lambda\tau} + a_3 = 0, \tag{30}$$

where

$$a_1 = -\frac{\alpha x^* y^*}{(h+x^*)^2} = -\left(\frac{m+E_2}{\beta}\right)\left(r - \frac{r(m+E_2)h}{K(\beta - m - E_2)}\right),$$

$$a_2 = \frac{rx^*}{K} = \frac{r(m+E_2)h}{K(\beta - m - E_2)},$$

$$a_3 = \frac{h\alpha\beta x^* y^*}{(h+x^*)^3} = \left(\frac{m+E_2}{\beta}\right)(\beta - m - E_2)\left(r - \frac{r(m+E_2)h}{K(\beta - m - E_2)}\right).$$

Since we have already attempted to attain stability in the system under unharvested and non-delayed case (Section 3.1), here, we deal with the delayed and harvested case.

Now for $\tau \neq 0$, let us suppose there exist $\lambda = i\omega$ ($\omega > 0$). The characteristics Eq. (30) can be written as, (separating the real and imaginary parts)

$$-\omega^2 + \omega a_2 \sin(\omega\tau) + a_3 = 0, \tag{31a}$$

$$a_1\omega + a_2\omega\cos(\omega\tau) = 0. \tag{31b}$$

Let us define,

$$\theta_1 = \arccos\left(-\frac{a_1}{a_2}\right), 0 < \theta_1 < \frac{\pi}{2},$$

$$\theta_2 = \arccos\left(-\frac{a_1}{a_2}\right), \frac{3\pi}{2} < \theta_2 < 2\pi.$$

Accordingly, for the choice of $\theta_1$ and $\theta_2$, we get two positive values of $\omega$ given as,

$$\omega_+ = \frac{1}{2}\sqrt{a_2^2 - a_1^2} + \frac{1}{2}\sqrt{a_2^2 - a_1^2 + 4a_3}, \tag{32}$$

$$\omega_- = -\frac{1}{2}\sqrt{a_2^2 - a_1^2} + \frac{1}{2}\sqrt{a_2^2 - a_1^2 + 4a_3}. \tag{33}$$

provided $a_2^2 - a_1^2 + 2a_3 > 0$ and $(a_2^2 - a_1^2 + 2a_3) > 4a_3^2$. The corresponding $\tau$ will be given as,

$$\tau_n^+ = \frac{\theta_1 + 2n\pi}{\omega_+},$$

$$\tau_n^- = \frac{\theta_2 + 2n\pi}{\omega_-}.$$

We get different set of values of $\tau_n^{\pm}$ based on the different effort of harvesting $E_2$.

## References


[1] Abrams PA, Roth JD. The effects of enrichment of three-species food chains with nonlinear functional responses. Ecology 1994;75(4):1118–30.
[2] Beddington JR, May RM. Time delays are not necessarily destabilizing. Math Biosci 1975;27(1–2):109–17.
[3] Beddington JR, May RM. Maximum sustainable yields in systems subject to harvesting at more than one trophic level. Math Biosci 1980;51(3):261–81.
[4] Chen Y, Zhang F. Dynamics of a delayed predator–prey model with predator migration. Appl Math Model 2013;37(3):1400–12.
[5] Cooke KL, Grossman Z. Discrete delay, distributed delay and stability switches. J Math Anal Appl 1982;86(2):592–627.
[6] Dunn RP, Baskett ML, Hovel KA. Interactive effects of predator and prey harvest on ecological resilience of rocky reefs. Ecol Appl 2017;27(6):1718–30.
[7] Freedman H, Gopalsamy K. Global stability in time-delayed single-species dynamics. Bull Math Biol 1986;48(5–6):485–92.
[8] Geček S, Legović T. Impact of maximum sustainable yield on competitive community. J Theor Biol 2012;307:96–103.
[9] Ghosh B, Kar TK. Possible ecosystem impacts of applying maximum sustainable yield policy in food chain models. J Theor Biol 2013;329:6–14.
[10] Ghosh B, Kar TK, Legović T. Relationship between exploitation, oscillation, MSY and extinction. Math Biosci 2014;256:1–9.
[11] Ghosh B, Kar TK, Legović T. Sustainability of exploited ecologically interdependent species. Popul Ecol 2014;56(3):527–37.
[12] Ghosh B, Pal D, Kar TK, Valverde JC. Biological conservation through marine protected areas in the presence of alternative stable states. Math Biosci 2017;286:49–57.
[13] Ghosh B, Pal D, Legović T, Kar TK. Harvesting induced stability and instability in a tri-trophic food chain. Math Biosci 2018;304:89–99.
[14] Gourley SA, Kuang Y. A stage structured predator–prey model and its dependence on maturation delay and death rate. J Math Biol 2004;49(2):188–200.
[15] Hastings A, Powell T. Chaos in a three-species food chain. Ecology 1991;72(3):896–903.
[16] Hilborn R. Pretty good yield and exploited fishes. Mar Policy 2010;34(1):193–6.
[17] Ho CP, Ou YL. Influence of time delay on local stability for a predator–prey system. J Tunghai Sci 2002;4:47–62.
[18] Hutchinson GE. Circular causal systems in ecology. Ann N Y Acad Sci 1948;50(4):221–46.
[19] Juneja N, Agnihotri K, Kaur H. Effect of delay on globally stable prey–predator system. Chaos, Solitons Fractals 2018;111:146–56.
[20] Kar TK. Stability analysis of a prey–predator model with delay and harvesting. J Biol Syst 2004;12(01):61–71.
[21] Kar TK, Ghorai A. Dynamic behaviour of a delayed predator–prey model with harvesting. Appl Math Comput 2011;217(22):9085–104.
[22] Kar TK, Ghosh B. Sustainability and optimal control of an exploited prey–predator system through provision of alternative food to predator. Biosystems 2012;109(2):220–32.
[23] Kar TK, Ghosh B. Sustainability and economic consequences of creating marine protected areas in multispecies multiactivity context. J Theor Biol 2013;318:81–90.
[24] Kar TK, Pahari UK. Non-selective harvesting in prey–predator models with delay. Commun Nonlinear Sci Numer Simul 2006;11(4):499–509.
[25] Klebanoff A, Hastings A. Chaos in one-predator, two-prey models: cgeneral results from bifurcation theory. Math Biosci 1994;122(2):221–33.
[26] Kundu S, Maitra S. Dynamical behaviour of a delayed three species predator–prey model with cooperation among the prey species. Nonlinear Dyn 2018;92(2):627–43.
[27] Legović T. When is the phytoplankton biomass a reliable indicator of eutrophication. Nova Thalassia 1979;3:323–33.
[28] Legović T. Impact of demersal fishery and evidence of the Volterra principle to the extreme in the Adriatic Sea. Ecol Modell 2008;212(1–2):68–73.
[29] Legović T, Klanjšček J, Geček S. Maximum sustainable yield and species extinction in ecosystems. Ecol Modell 2010;221(12):1569–74.
[30] Li H, Meng G, She Z. Stability and Hopf bifurcation of a delayed density-dependent predator–prey system with Beddington–DeAngelis functional response. Int J Bifurcation Chaos 2016;26(10):1650165.
[31] Li H, Takeuchi Y. Dynamics of the density dependent predator–prey system with Beddington–DeAngelis functional response. J Math Anal Appl 2011;374(2):644–54.
[32] Liu C, Lu N, Zhang Q, Li J, Liu P. Modeling and analysis in a prey–predator system with commercial harvesting and double time delays. Appl Math Comput 2016;281:77–101.
[33] Liu C, Zhang Q, Li J, Yue W. Stability analysis in a delayed prey–predator-resource model with harvest effort and stage structure. Appl Math Comput 2014;238:177–92.
[34] Liu W, Jiang Y. Bifurcation of a delayed Gause predator–prey model with Michaelis–Menten type harvesting. J Theor Biol 2018;438:116–32.
[35] Martin A, Ruan S. Predator–prey models with delay and prey harvesting. J Math Biol 2001;43(3):247–67.

[36] Matsuda H, Abrams PA. Maximal yields from multispecies fisheries systems: rules for systems with multiple trophic levels. Ecol Appl 2006;16(1):225–37.
[37] May RM, Beddington JR, Clark CW, Holt SJ, Laws RM. Management of multispecies fisheries. Science 1979;205(4403):267–77.
[38] Meng X, Huo H, Zhang X. The effects of harvesting and time delay on predator–prey systems with Beddington–DeAngelis functional response. Int J Biomath 2012;5(01):1250008.
[39] Misra AK, Dubey B. A ratio-dependent predator–prey model with delay and harvesting. J Biol Syst 2010;18(02):437–53.
[40] Nicholson AJ. An outline of the dynamics of animal populations. Aust J Zool 1954;2(1):9–65.
[41] Pikitch EK, Santora C, Babcock EA, Bakun A, Bonfil R, Conover DO, et al. Ecosystem-based fishery management. Science 2004;305(5682):346–7.
[42] Pilyugin SS, Medlock J, De Leenheer P. The effectiveness of marine protected areas for predator and prey with varying mobility. Theor Popul Biol 2016;110:63–77.
[43] Rosenzweig ML, MacArthur RH. Graphical representation and stability conditions of predator–prey interactions. Am Nat 1963;97(895):209–23.
[44] Roy B, Roy SK, Gurung DB. Holling–Tanner model with Beddington–DeAngelis functional response and time delay introducing harvesting. Math Comput Simul 2017;142:1–14.
[45] Schaefer MB. Some aspects of the dynamics of populations important to the management of the commercial marine fisheries. Inter-Am Tropical Tuna Commission Bull 1954;1(2):23–56.
[46] Shi R, Yu J. Hopf bifurcation analysis of two zooplankton-phytoplankton model with two delays. Chaos, Solitons Fractals 2017;100:62–73.
[47] Shu H, Hu X, Wang L, Watmough J. Delay induced stability switch, multitype bistability and chaos in an intraguild predation model. J Math Biol 2015;71(6–7):1269–98.
[48] Toaha S, Hassan MA. Stability analysis of predator–prey population model with time delay and constant rate of harvesting. Punjab Univ J Math 2008;40:37–48.
[49] Toaha S, Hassan MHA, Ismail F, June LW. Stability analysis and maximum profit of predator–prey population model with time delay and constant effort of harvesting. Malaysian J Math Sci 2008;2(2):147–59.
[50] Tromeur E, Doyen L. Optimal biodiversity erosion in multispecies fisheries. Tech. Rep. Groupe de Recherche en Economie Théorique et Appliquée; 2016.
[51] Tromeur E, Loeuille N. Balancing yield with resilience and conservation objectives in harvested predator–prey communities. Oikos 2017;126(12):1780–9.
[52] Wang X, Zou X. Modeling the Fear effect in predator–prey interactions with adaptive avoidance of predators. Bull Math Biol 2017;79(6):1325–59.
[53] Wang Y, Tu Q. Multiple positive periodic solutions for a delayed predator–prey system with Beddington–DeAngelis functional response and harvesting terms. Ann Univ Craiova-Math Comput Sci Ser 2015;42(2):330–8.
[54] Xia J, Liu Z, Yuan R, Ruan S. The effects of harvesting and time delay on predator–prey systems with Holling type II functional response. SIAM J Appl Math 2009;70(4):1178–200.
[55] Zhang H, Xia J, Georgescu P. Multigroup deterministic and stochastic SEIRI epidemic models with nonlinear incidence rates and distributed delays: a stability analysis. Math Methods Appl Sci 2017;40(18):6254–75.
[56] Zhang H, Xia J, Georgescu P. Stability analyses of deterministic and stochastic SEIRI epidemic models with nonlinear incidence rates and distributed delay. Nonlinear Anal 2017;22(1):64–83.
[57] Zhang JF. Bifurcation analysis of a modified Holling–Tanner predator–prey model with time delay. Appl Math Model 2012;36(3):1219–31.